UNCLASSIFIED

AD NUMBER: AD0842808
LIMITATION CHANGES
TO: Approved for public release; distribution is unlimited.
FROM: Distribution authorized to US Government Agnecies and their Contractors; Export Control; 14 Aug 1968. Other requests shall be referred to US Army Missile Command, Redstone Arsenal, AL 35809.
AUTHORITY
USAMC ltr dtd 23 Aug 1971

THIS PAGE IS UNCLASSIFIED

AD

AD842808

REPORT NO. RG-TR-68-11

THE EFFECT OF NEUTRON RADIATION ON UNIJUNCTION TRANSISTORS AND SILICON CONTROL RECTIFIERS

by

Victor W. Ruwe

August 1968

This document is subject to special export controls and each transmittal to foreign governments or foreign nationals may be made only with prior approval of this Command. ATTN: AMSMI-RG.

U.S. ARMY MISSILE COMMAND

Redstone Arsenal, Alabama

DDC

NOV 8 1968

A

94

14 August 1968

Report No. RG-TR-68-11

THE EFFECT OF NEUTRON RADIATION ON UNIJUNCTION TRANSISTORS AND SILICON CONTROL RECTIFIERS

by

Victor W. Ruwe

This document is subject to special export controls and each transmittal to foreign governments or foreign nationals may be made only with prior approval of this Command. ATTN: AMSMI-RG.

Army Missile Comd.
Redstone Arsenal Ala. 35809

Electrical Systems Branch
Army Inertial Guidance and Control Laboratory and Center
Research and Development Directorate
U. S. Army Missile Command
Redstone Arsenal, Alabama 35809

ABSTRACT

Presented in this paper are the results of theoretical study and of actual tests on unijunction transistors in a nuclear environment of fast neutrons. The investigation of Silicon Control Rectifiers was principally restricted to their use with unijunction transistors.

In the theoretical study, a technique was developed to predict damage caused by neutrons. A number of sample unijunction transistors were irradiated, then tested, and the results compared with predicted values. It was found that the construction of the device was important in determining the level of radiation that the device could withstand. This study indicates that the monolithic device can be expected to operate in neutron environments about five times higher than the bar type device and the Silicon Control Rectifiers.

FOREWORD

This paper was previously published as a master's thesis at the University of Alabama in Huntsville. The work was conducted at the White Sands Missile Range and at Redstone Arsenal. At the termination of the study, a rough draft was submitted to the University of Alabama and was accepted as a master's thesis subject.

ACKNOWLEDGEMENT

The author would like to express his gratitude to Dr. J. C. Dowdle for his assistance and patience with the preparation of this paper.

BLANK PAGE

CONTENTS

Page

Chapter I. INTRODUCTION 1

Chapter II. THEORY OF SOLID-STATE DEVICES AS RELATED TO RADIATION DAMAGE 4

A. General Theory of Solid-State Devices 4
B. The Unijunction Transistor 14

Chapter III. PREDICTED RADIATION DAMAGE 17

A. Unijunction Transistor Damage 17
B. Silicon Control Rectifier Damage 40

Chapter IV. PROCEDURE AND RESULTS OF RADIATION TEST 43

A. Irradiating Procedure 43
B. Results 44

Chapter V. EFFECT ON CIRCUIT DESIGN 65

Chapter VI. CONCLUSIONS 72

Appendix. CHARACTERISTIC CURVE FITTING FOR THE SILICON CONTROL RECTIFIER 75

REFERENCES 77

ILLUSTRATIONS

Table		Page
I	Irradiation Levels	44
A-I	Input Data for Silicon Control Rectifier Curve Fittings	75
A-II	Output Data for Three Terms	76
A-III	Output Data for Four Terms	76
A-IV	Output Data for Five Terms	76

Figure		Page
1	Physical Model of Unijunction Transistor	14
2	Network Analogy Model of Unijunction Transistor	15
3	Saturation Resistance Model	17
4	Charge Distribution in the Unijunction	18
5	Bar Unijunction Transistor with Dimensions	19
6	Unsaturated Resistance as a Function of Current for Bar-Type Unijunction	22
7	Circuit for Measuring Characteristics Curves	23
8	Saturated Resistance as a Function of Current for Bar-Type Unijunction	24
9	Composite Curve for Bar Type Unijunction	25
10	Voltage-Current Characteristic Curve for Bar Type Unijunction	26

Figure		Page
11	Saturated Resistance for Bar-Type Unijunction 1.71×10^{12} Neutrons per Square Centimeter	27
12	Unsaturated Resistance for Bar-Type Unijunction 1.7×10^{12} Neutrons per Square Centimeter	28
13	Composite Curve for Bar-Type Unijunction 1.7×10^{12} Neutrons per Square Centimeter	29
14	Voltage-Current Characteristic Curve for Bar-Type Unijunction 1.7×10^{12} Neutrons per Square Centimeter	30
15	Monolithic Type Construction	33
16	Effective Model of Monolithic Unijunction	34
17	Characteristic Curve for Monolithic-Type Unijunction	36
18	Voltage-Current Characteristic Curve for Monolithic-Type Unijunction	37
19	Characteristic Curve for Monolithic-Type Unijunction 7.3×10^{12} Neutrons per Square Centimeter	38
20	Voltage-Current Characteristic Curve for Monolithic-Type Unijunction 7.3×10^{12} Neutrons per Square Centimeter	39
21	Mounting Configuration	43
22	Bar-Type Unijunction Without Radiation	45
23	Bar-Type Unijunction with 1.7×10^{12} Neutrons per Square Centimeter	46
24	Bar-Type Unijunction with 7.3×10^{12} Neutrons per Square Centimeter	47
25	2N3980 Voltage-Current Characteristics for No Radiation	48

Figure | Page

26 2N3980 Voltage-Current Characteristics for 1.73×10^{12} Neutrons per Square Centimeter 48

27 2N3980 Voltage-Current Characteristics for 7.3×10^{12} Neutrons per Square Centimeter 49

28 2N3480 Voltage-Current Characteristics for No Radiation 49

29 2N3480 Voltage-Current Characteristics for 1.7×10^{12} Neutrons per Square Centimeter 50

30 2N3480 Voltage-Current Characteristics for 7.3×10^{12} Neutrons per Square Centimeter 50

31 Modified Equivalent Circuit 51

32 Corrected Characteristic Curve for Bar-Type Unijunction 52

33 Corrected Voltage-Current Characteristic Curve for Bar-Type Unijunction 53

34 Corrected Characteristic Curve for Bar-Type Unijunction 1.7×10^{12} Neutrons per Square Centimeter 54

35 Corrected Voltage-Current Characteristic Curve for Bar-Type Unijunction 1.7×10^{12} Neutrons per Square Centimeter 55

36 Corrected Composite Curve for Monolithic-Type Unijunction 56

37 Corrected Voltage-Current Characteristic Curve for Monolithic-Type Unijunction 57

38 Corrected Composite Curve for Monolithic-Type Unijunction 7.3×10^{12} Neutrons per Square Centimeter 58

39 Corrected Voltage-Current Characteristic Curve for Monolithic-Type Unijunction 7.3×10^{12} Neutrons per Square Centimeter 59

SYMBOLS

A	area (cm^2)
b	ratio of the electron to base mobility
D	diffusion constant (cm^2/sec)
D_n	electron diffusion constant (cm^2/sec)
D_p	hole diffusion constant (cm^2/sec)
E	energy
$f_{(t)}$	current-gain bandwidth product
g	thermal carrier generation rate (carriers/cm^3-sec)
g_o	radiation carrier generation constant in silicon (4×10^{13} carriers/cm^3-rad)
H_{fe}	DC common emitter current gain
H_{fen}	DC common emitter current gain of the P-N-P transistor of a Silicon Control Rectifier
H_{fep}	DC common emitter current gain of the N-P-N transistor of a Silicon Control Rectifier
I	current (A)
I_A	silicon controlled rectifier anode current (A)
I_B	base current (A)
I_n	electron current (A)

Figure		Page

40 Current-Dose Curve for 2N1772 Silicon Control Rectifier 60

41 Current-Dose Curve for 2N1843 Silicon Control Rectifier 61

42 Current Dose Curve for 2N1595 Silicon Control Rectifier 62

43 General Prediction Curve for Silicon Control Rectifiers 63

44 Time Circuit 65

45 Corrected Unijunction Model 66

46 Capacitor Discharge Curve for Nonradiated Case Bar-Type Unijunction 67

47 Relaxation Oscillator 68

48 Input Wave Shape 68

49 Change in Operational Characteristic for Unijunction with Changes in Supply Voltage 71

I_p	hole current (A)
K	radiation damage constant, effective change in the recombination rate per neutron/cm^2 exposure (cm^2/n-sec)
K_o	radiation damage constant at low injection (cm^2/n-sec)
K_{rg}	radiation damage constant in a diode junction (cm^2/n-sec)
K_∞	radiation damage constant at high injection (cm^2/n-sec)
k	Boltzmann's constant (1.38×10^{-23} J/deg)
L	diffusion length (cm)
ℓ	length
m	base field parameter
N	impurity concentration (atoms/cm^3)
N_A	acceptor impurity concentration (atoms/cm^3)
N_D	donor impurity concentration (atoms/cm^3)
N_i	intrinsic carrier concentration (carriers/m^3)
N_n	electron concentration in the N region (cm^{-3})
N_o	number of samples in a normal distribution
N_p	doping level
N_{po}	thermal equilibrium electron concentration in P region (cm^{-3})
P	hole concentration or density (cm^{-3})
P_{no}	thermal equilibrium hole concentration (cm^{-3})
P_p	hole concentration in P region (cm^{-3})
q	charge of an electron (C/electron)
R	recombination rate per carrier (sec^{-1})
R_N	recombination rate per carrier for N-type material

R_o	pre-irradiation recombination rate per carrier (sec^{-1})
rad	the amount of radiation which deposits 100 ergs/g in a specific material (silicon)
r_{sc}	collector body resistance (ohms)
T	absolute temperature (°K)
t_{bp}	base transit time(s) for PNP transition
t_{bn}	base transit time(s) for NPN transition
t	time (sec)
t_b	base transit time (sec)
V	voltage
V_{bb}	external base voltage (V)
V_d	junction voltage
V_e	unijunction transistor firing voltage
V_o	carrier velocity
W	region width
ΔN	excess electron carrier concentration (cm^{-3})
ΔP	excess hole concentration (cm^{-3})
ϵ	electric field (V/cm)
ϵ_o	permittivity of silicon (F/cm)
λ	wavelength of light (cm)
μ_n	electron mobility (cm^2/V-sec)
μ_o	mobility (cm^2/V-sec)
μ_p	hole mobility (cm^2/V-sec)
ρ	resistivity (ohms)

σ	conductivity (ohm-cm^{-1})
τ	minority carrier lifetime (sec)
τ_n	minority carrier lifetime for electrons in the P region (sec)
τ_o	lifetime before irradiation (10^{-1} sec)
ϕ	time integrated neutron flux (or fluence) (c/cm^2)

BLANK PAGE

CHAPTER I

INTRODUCTION

The field of neutron irradiation is a fairly new field of endeavor. The first observation of the neutron took place in 1930 and was observed by Bothe and Becher [1]. At this time, a highly penetrating radiation was found when beryllium was bombarded with alpha particles. This radiation was thought to be a very short wavelength gamma ray. Not until 1932 did Chadwick [1] show that this radiation was a neutrally charged particle called a neutron. This discovery did not have an impact on engineering because at this time the only source of neutrons was limited to laboratory generation.

With the advent of nuclear reactors in 1943 [2] and the atomic bomb in 1945, the neutron environment became a problem to be considered. Due to the highly penetrating characteristics of neutrons, no adequate way of shielding has been developed other than that which is prohibitive. A number of studies were conducted between 1945 and 1960 to determine the effects of radiation, and The Transient Radiation Effect on Electronics Handbook [3] is a summation of work done during this period. From these studies it was found that electronic equipment employing vacuum tubes could survive in higher levels of neutron radiation than man could endure. No appreciable work was done on electronics

in a neutron environment until the advent of transistors which were developed by Bell Telephone Laboratory in 1948 [4]. These devices depend on a very uniform crystalline structure which is very susceptible to damage from neutrons [5].

During the ten-year period from 1948 to 1958, semiconductor devices came into widespread use. During this same period both the engineers and physicists became interested in the effects of neutron damage to semiconductor devices. The engineering community studied the effects on particular devices as exemplified by The Boeing Company [6-9], while the physicists studied the damage mechanism in the semiconductor material.

In 1951 James and Lark-Horavitz developed a defect-energy-level model [10] which permitted work on the effect of neutrons on the conductivity of semiconductor material, and Vovilov [11] worked in the minority carrier lifetime. In 1962 [12] these two disciplines were merged. Larin [13] of Bendix Company, using this combination, developed a technique for predicting radiation effect.

The work in this thesis is closely aligned with the work done by Larin. The technique for predicting damage to transistors and diodes is used as a model to develop a technique to predict displacement damage to unijunction transistors caused by neutrons. To evaluate this technique, a number of devices were irradiated and the results compared with these predictions.

In this paper a technique is developed that allows the prediction of changes in the operating characteristics of the unijunction transistor and the

Silicon Control Rectifier (SCR) due to neutron irradiation. A network model is developed for the unijunction transistor, and this model is compared with empirical data and then modified to account for the differences. This network model is then used in predicting circuit operations.

CHAPTER II

THEORY OF SOLID-STATE DEVICES AS RELATED TO RADIATION DAMAGE

A. General Theory of Solid-State Devices

The devices considered in this paper were made of a silicon base semiconducting material. In order to facilitate the discussion of these devices, a brief presentation of solid-state theory is included as developed by Van der Ziel's [14] interpretation of radiation. Larin's damage theory [13] is also included.

The four electrons in the outer shell of silicon are shared with other atoms in covalent bonds. These electrons are usually found in the valence band, but energy can be added to drive these electrons into the conduction band. Energy to raise the electrons to the conduction band can originate from a number of sources. The most important of these sources are thermal, electro-magnetic, and nuclear radiation. When an electron is raised to the conduction band, a positive charge (hole) is left by the absence of the electron. Two current carriers are then available and such a process is termed hole-electron pair generation. The reverse action is called recombination.

In pure uncharged silicon, the number of electrons must equal the number of holes and is given as

$$N_i = 3.87 \times 10^{16} (T)^{3/2} e^{-\frac{1.21}{2kt}} . \qquad (2\text{-}1)$$

The number of carriers available is directly dependent on the temperature, and the carrier concentration for a particular temperature is dependent on the dopant added to the silicon. Both P and N types of doping material are commonly used. The N type dopant causes the silicon to have an excess of electrons whereas the P type produces an excess of holes.

If the case is considered where a chip of silicon has been doped with an element to produce an excess of electrons and there is sufficient energy available for these electrons to be in the conduction band, the electrons in the conduction band can then be attributed directly to the doping element. A large number of electrons results, which consequently raises the recombination rate. Since N_i must remain constant, the number of holes is reduced from the intrinsic value as indicated by the following relation:

$$N_i = [\text{(number of holes)(number of electrons)}]^{1/2} . \qquad (2\text{-}2)$$

Equation (2-2) applies for both intrinsic or doped silicon.

Imperfections in the silicon crystal lattice allow electrons to obtain energy levels which lie between the valence band and the conduction band which is called the "forbidden band." These imperfections can be built in at the time of manufacture or can be caused by radiation displacement damage. These imperfections or defects are the center of hole-electron pair generation and/or recombination. The lifetime of a carrier (hole or electron) is dependent on the number of these defects in the silicon lattice.

This is an important concept because the carrier lifetime is proportional to the number of defects and in turn to the radiation dose received. The Shockley-Read-Hall [13] theory is used to determine the electrical behavior of these defects. The equation can be written for electrons in P type material as [13]

$$\frac{dN}{dt} = g - \frac{N_p}{\tau_n} = g - N_p R_n \quad . \tag{2-3}$$

At thermal equilibrium

$$\frac{dN}{dt} = 0$$

and the minority carrier concentration N_{po} is given as

$$N_{po} = \frac{g}{R_n} \quad . \tag{2-4}$$

The nonequilibrium condition of minority carriers conforms to the following equation

$$\frac{dN}{dt} = g - \frac{N_{po} + \Delta N}{\tau_n} = \frac{\Delta N}{\tau_n} \tag{2-5}$$

where

$$\Delta N = N_p - N_{po}$$

and a solution to equation (2-5) can be shown to be

$$\Delta N(t) = \Delta N_o e^{-\frac{t}{\tau_n}} \quad . \tag{2-6}$$

At $t = 0$, $\Delta N = \Delta N_o$.

Equation (2-6) permits the prediction of radiation effects on recombination and generation rates in a silicon base. Defects thus indicate a measure of neutron damage. The number of defects produced by radiation is proportional to radiation cumulative dose. After irradiation the recombination rate per carrier can be expressed as [13]

$$R = R_o + K\phi \ . \tag{2-7}$$

The radiation damage coefficient K is appropriately named "coefficient" because it varies from device to device and is dependent on doping levels, temperature, and radiation energy. A device which depends on a low rate of recombination would be seriously affected by radiation.

The motions of carriers through semiconductors are of two types, diffusion and drift. Carrier diffusion is random and takes place in the absence of an electric field. The type of motion that occurs in the presence of an electric field is called drift.

The velocity of the carrier in the electric field is given as

$$V_o = \mu_o \epsilon \ . \tag{2-8}$$

The mobility is a function of doping levels.

When the electric field becomes excessively large, the velocity reaches a maximum of 8.5×10^6 centimeters per second; however, in most devices, the fields are sufficiently small to prohibit the velocity from nearing saturation.

The current passing through an area A can be expressed as

$$I_n = qAN\mu_n \epsilon \tag{2-9}$$

for electrons and

$$I_p = qAP\mu_p\epsilon \qquad (2\text{-}10)$$

for holes.

The total current due to the motion of both holes and electrons can be expressed as the sum of equations (2-9) and (2-10)

$$I = I_n + I_p \qquad (2\text{-}11)$$

$$I = qA\left(\mu_n N + \mu_p P\right)\epsilon \ . \qquad (2\text{-}12)$$

Since $\epsilon = V/\ell$, where ℓ is the length and V is the applied voltage, the current can be expressed as

$$I = qA\left(\mu_n N + \mu_p P\right)\frac{V}{\ell} \ . \qquad (2\text{-}13)$$

The resistance of the silicon can be calculated by rearranging equation (2-13).

$$R = \frac{V}{I} = \frac{1}{q\left(\mu_n N + \mu_p P\right)} \qquad (2\text{-}14)$$

From the simple equation defining resistance for a uniform geometry of resistivity ρ

$$R = \frac{\rho\ell}{A} \ , \qquad (2\text{-}15)$$

and equation (2-14) the resistivity can be determined to be

$$\rho = \frac{1}{q\left(\mu_n N + \mu_p P\right)} \qquad (2\text{-}16)$$

In the absence of an electric field, the current is proportional to the gradient of the carrier concentration. The electron current is a linear

function of gradient and is given as

$$I_n = qAD\frac{dN}{dX} \tag{2-17}$$

where D is the diffusion constant. The diffusion constant is similar to mobility in that they both describe the carrier's ability to move through the medium. These two constants are related to each other by Einstein's equation

$$D = \mu\left(\frac{kT}{q}\right) . \tag{2-18}$$

The concept that is important to this study is the diffusion length. The diffusion length is the distance that the minority carrier can travel before it recombines with a major carrier. This is expressed as

$$L^2 = D\tau . \tag{2-19}$$

It is significant to describe the operation of a diode. Important in the understanding of the diode operation is the involvement of the diffusion current at the junction boundary. This current at the boundary can be determined if the gradient of the minority carrier concentration is known. The minority carrier concentration is computed by use of the Boltzmann relation. The diode behavior can be calculated from

$$I\Big|_{X = 0} = qAD_n \frac{dN}{dX}\Bigg|_{X = 0} \tag{2-20}$$

where X is the displacement from the junction.

The differential equation for the carrier concentration as a function of time can be written as

$$\frac{dN}{dt} = D\frac{d^2N}{dX^2} - \frac{\Delta N}{\tau} = 0 \qquad (2\text{-}21)$$

where the electric field ϵ is zero.

The solution to equation (2-21) is a complex hyperbolic function which can be simplified for two cases. In the first case, the width W is large in comparison with the diffusion length L, and in the second case, the width is small. The first case has an exponential solution, whereas the second has a linear solution.

Equations (2-20) and (2-21) have solutions which reduce to

$$I_n = qAD_n \frac{\Delta N}{L} \qquad (2\text{-}22)$$

where L ≪ W.

$$I_n = qAD_n \frac{\Delta N}{W} \qquad (2\text{-}23)$$

where W ≪ L.

Equation (2-22) can be combined with the general diode equation,

$$\Delta N = N_{po}\left(e^{\frac{qV_d}{kt}} - 1\right) \qquad (2\text{-}24)$$

to yield

$$I_n = \frac{qAD_n N_{po}}{W_n}\left(e^{\frac{qV_d}{kt}} - 1\right) \qquad (2\text{-}25a)$$

and

$$I_p = \frac{qAD_p P_{no}}{W_p}\left(e^{\frac{qV_d}{kt}} - 1\right). \qquad (2\text{-}25b)$$

By adding equations 2-25a and 2-25b equation 2-26 is obtained.

$$I = qA\left(\frac{D_p N_{po}}{W_p} + \frac{D_n P_{no}}{W_n}\right)\left(e^{\frac{qV_d}{kt}} - 1\right) . \quad (2\text{-}26)$$

In power diodes, the width is not small in comparison with the diffusion length, and the equation for I must be modified by replacing W with the appropriate diffusion length L.

In many applications, the next logical item of discussion is the low current injection mode; however, in the application of this paper only the high current injection mode need be considered. The difference between low injection and high injection is the relation between the number of minority carriers and the impurity concentration. When the number of carriers approaches the impurity concentration, the device goes into the high injection mode.

There is one high injection characteristic that is of particular interest in the study of unijunction transistors and SCR's in a neutron environment, saturation resistance. The number of minority carriers controls this characteristic and is affected directly by radiation.

The conductivity of a silicon device can be expressed as [14]

$$\sigma = q\left(\mu_n N + \mu_p P\right) . \quad (2\text{-}27)$$

Although this is a low injection equation, it can be modified for high injection. At high injection, an increase in the minority carriers causes an increase in majority carriers. The above equation can be modified to read:

$$\sigma = q\left[\mu_n \Delta N + \mu_p\left(N_A + \Delta N\right)\right] , \quad (2\text{-}28)$$

or

$$\sigma = q\left[\mu_p \Delta P + \mu_n\left(N_D + \Delta P\right)\right] , \quad (2\text{-}29)$$

depending on the type of semiconductor material.

Since

$$\frac{\mu_n}{\mu_p} \cong 2.5 ,$$

equation (2-29) can be reduced to

$$\sigma = \sigma_o + 1.4\, q\mu_n \Delta N , \quad (2\text{-}30)$$

where σ_o is the low injection conductivity.

It then follows that the resistivity can be expressed as

$$\rho = \frac{1}{\sigma_o + 1.4\, q\mu_n \Delta N} . \quad (2\text{-}31)$$

Because of the uniform geometry of the semiconductor material, its resistance can be conveniently expressed as

$$\text{Resistance} = \frac{\rho L}{A} .$$

The unijunction transistor power diodes and SCR's are operated in the high injection mode. A unijunction transistor operates in a manner similar to that of a power diode. The voltage drop across a power diode conducting in the forward direction is a function of doping levels, current, and diffusion length. If the diffusion length is long in comparison with the width of the region, the diode can be expected to have a low voltage drop. The voltage can then be expressed as

$$V = \frac{2kt}{q} \, Ln \, \frac{IW}{2qADN_i} \; . \qquad (2\text{-}32)$$

As diffusion length is decreased, the current that the diode is carrying must pass through a resistance. The diffusion length is then a direct function of minority carrier lifetime.

$$L^2 = D_n \tau_n \qquad (2\text{-}33)$$

When τ_n is the minority carrier lifetime, a transistor can be considered as two back-to-back diodes and consists of three layers of doped silicon.

For the purpose of the following discussion, an N-P-N transistor is chosen for consideration. A junction which forms a diode exists between each of the areas. The purpose of such a three-layer device is to control a large current from the emitter to collector with a small base current. Electrons must move from the N region at the emitter to the N region at the collector without recombining in the base. The time for this transition is called the base transit time t_b. Multiplication of base transit time and recombination rate yields the probability of recombination occurring [13].

The common emitter gain H_{fe} can then be expressed as

$$H_{fe} = \frac{1}{t_b R_n} - 1 \; . \qquad (2\text{-}34)$$

As a function of neutron radiation H_{fe} can be expressed as

$$H_{fe} = \frac{1}{t_b \left(R_o + k\phi \right)} - 1 \; . \qquad (2\text{-}35)$$

The current-gain bandwidth product f(t) is given as

$$f(t) = \frac{1}{2\pi t_b} , \qquad (2\text{-}36)$$

and is the frequency for which the common emitter current gain equals unity. These expressions are necessary for the discussion of SCR's.

B. The Unijunction Transistor

There are two general constructions of unijunction transistors, the monolithic and the bar types. Both types operate in similar manner. The unijunction transistor consists of a single diode junction with two ohmic contacts on the P or N type material.

For the sake of simplicity, consider the unijunction to be constructed as shown in Figure 1. The P type material is implanted in the N type material at a point such that ℓ_1 is about 80 percent of ℓ_2. This forms the single diode junction which is treated as a point contact. If a voltage V_{bb} is applied between contacts B2 and B1, an electric field is established between the ohmic contacts.

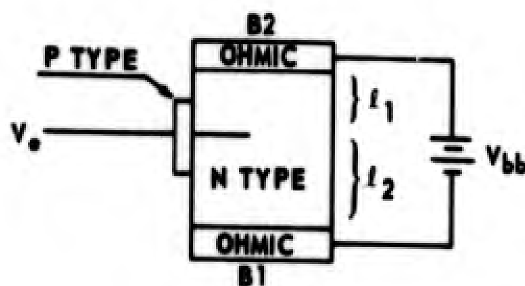

Figure 1. Physical Model of Unijunction Transistor

A voltage V_f is produced at the junction as a result of this applied field and is dependent on the relation of ℓ_2 and ℓ_1. This voltage can be expressed as

$$V_f = \frac{R_2 V_{bb}}{R_1 + R_2} \tag{2-37}$$

where

$$R_1 = \frac{\ell_1}{\sigma A} \text{ and } R_2 = \frac{\ell_2}{\sigma A} . \tag{2-38}$$

As long as the voltage applied to the P type material is less than V_f plus the built-in diode voltage V_d, current will not flow from the source driving V_e except for leakage. When the voltage applied to V_e reaches the same level as $V_f + V_d$, a current flows into the diode junction. This current causes holes to be injected into the N type material which reduces the resistance in the N type material, and, in turn, allows more holes to be injected. This process continues until the lower part of the N type material is flooded with injected holes, producing a condition termed saturation. The exact value of resistance that remains in the unsaturated area is dependent on the carrier's lifetime and injected hole current. The unijunction transistor in this configuration can be considered the same as the power diode case.

A network analogy model of this device is shown in Figure 2.

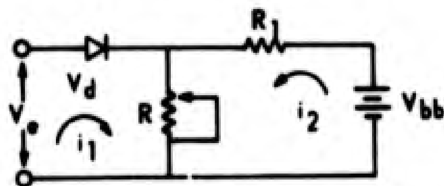

Figure 2. Network Analogy Model of Unijunction Transistor

The variable resistor R represents the resistance of the area to be saturated. The equations of this circuit are written as

$$+V_e = V_d + (i_1 - i_2)R$$

$$+V_{bb} = (i_2 - i_1)R + i_2R_1 \qquad (2\text{-}39)$$

where $R = 1.5$ kilohms and $V_d = 0.7$ volt.

It then follows that equation (2-39) can be solved for i_1, where K is 10^3.

$$i_1 = \frac{VR + 1.5kV - 0.7R - 0.7(1.5k) - V_{bb}R}{1.5kR} . \qquad (2\text{-}40)$$

Equation (2-40) can be used to obtain the value of V_e

$$V_e = \frac{i_1(1.5kR + 0.7R_2 + 1.05k + V_{bb}R_2)}{R_2 + 1.5k} . \qquad (2\text{-}41)$$

These network equations are combined with the damage equations in the next chapter producing the predicted operating characteristics.

CHAPTER III

PREDICTED RADIATION DAMAGE

A. Unijunction Transistor Damage

The unijunction transistor can be broken into four elements; these are the diode junction, resistance R_1, saturated resistance R_2, and unsaturated resistance R_3. The diode junction and resistance R_1 are affected by radiation but at much higher radiation levels than will affect the saturation resistance. In the following discussion, it is assumed that R_1 is fixed and that the junction voltage of the diode is also fixed at about 0.6 volt.

When a voltage is applied to the diode (Figure 3), and when this voltage reaches or exceeds the voltage developed across the N type material, the diode becomes forward biased and a current flows into the diode. This current causes holes to be injected into N type material. The number of holes injected and the diffusion length determines the value of R_2 and R_3. There was

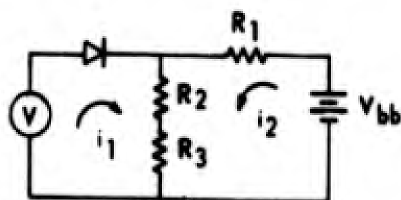

Figure 3. Saturation Resistance Model

an attempt to calculate the value of R_2 from the theory, but it did not result in a meaningful conclusion. This resistance was calculated from measured data. R_3 is caused by the unsaturated volume through which the combined currents flow. The holes injected by the diode current follow an exponential decay toward the ohmic contact B_1 where electrons are injected into the N type material; thus indicating that the hole concentration must fall off very quickly in this area (Figure 4). Hole concentration decay leaves an area of high resistance for the combined currents to flow through. Such high resistance is termed the unsaturated resistance and is indicated as R_3.

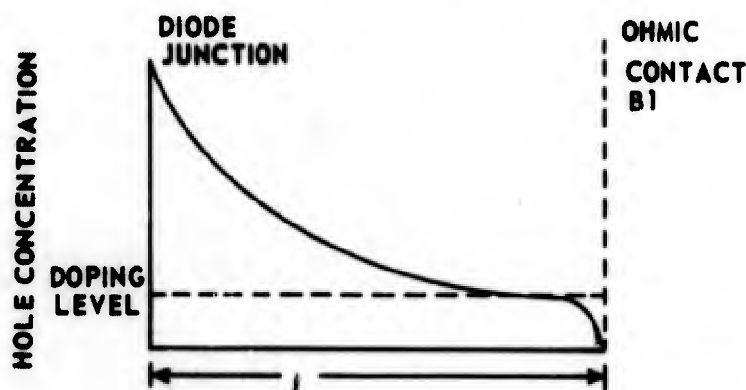

Figure 4. Charge Distribution in the Unijunction

Five 2N491B transistors were selected at random. One unit was disassembled, and its dimensions were measured. A sketch of the unit with the measurements is shown in Figure 5. All dimensions are in mils.

The intrinsic standoff ratio $\left(\frac{V_e}{V_{bb}}\right)$ was found to be 0.66 and the length 60 mils. When the diode voltage of 0.6 volt was removed, the length of the material available for saturation was calculated to be 36 mils. In the metric

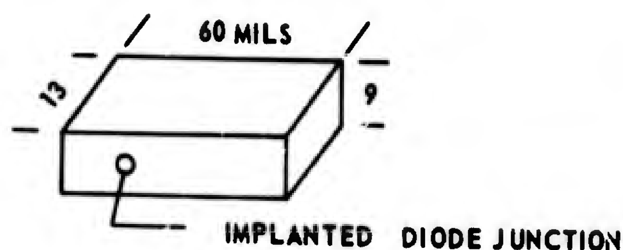

Figure 5. Bar Unijunction Transistor with Dimensions

system, the area is equal to 7.45×10^{-4} square centimeters and the length 9×10^{-2} centimeters.

The doping level N_p, 1.25×10^{14} atoms per square centimeter, and the lifetime τ, 10^{-4} seconds, were obtained from the material. From the graph in Larin's [13] paper, the mobility of the holes μ_p was found to be 0.5×10^3 square centimeters per volt-second. The diffusion constant can then be determined as

$$D_p = \frac{kT}{q}\mu_p = (0.026\ \mathrm{V})\left(\frac{500\ \mathrm{cm}^2}{\mathrm{V\text{-}sec}}\right) = 13\ \frac{\mathrm{cm}^2}{\mathrm{sec}} . \qquad (3\text{-}1)$$

The diffusion length can thus be calculated as

$$L_p = \left(D_p \tau\right)^{1/2} = (13 \times 10^{-4})^{1/2} = 3.6 \times 10^{-2}\ \mathrm{cm} . \qquad (3\text{-}2)$$

A comparison of the diffusion length, 3.6×10^{-2} centimeters, with the region available for saturation, 9.0×15^{-2} centimeters, shows that the diffusion length is the smaller.

It has been assumed that the concentration of holes at the point where the rapid decay begins is equal to the hole concentration that would exist at this point if there were no ohmic contact to disrupt the distribution.

The current injected at the diode junction was calculated and found to be

$$I = \frac{2qAD_p \Delta P_{(0)}}{L_p} \text{ amp} , \qquad (3\text{-}3)$$

where

$$q = 1.6 \times 10^{-19}$$

$$A = 7.45 \times 10^{-4} \text{ cm}^2$$

$$D_p = 13 \frac{\text{cm}^2}{\text{sec}} .$$

The concentration of injected holes $\left[\Delta P_{(0)}\right]$ can be expressed as

$$\Delta P_{(0)} = \frac{IL_p}{3.1 \times 10^{-21}} . \qquad (3\text{-}4)$$

The concentration of holes as shown in Figure 4 decreases exponentially and can be expressed as

$$P_{(X)} = \Delta P_{(0)} e^{-\frac{\ell}{1.2L_p}} . \qquad (3\text{-}5)$$

Equation (3-5) can then be used to calculate the apparent hole concentration at the ohmic contact

$$P_{(9 \times 10^{-2})} = \frac{IL_p}{3.1 \times 10^{-21}} e^{-\frac{0.09}{1.2L_p}} . \qquad (3\text{-}6)$$

It is first necessary that a determination be made of the length of the unsaturated region. In doing so, it is assumed that the decay from the injected hole concentration to the normal hole concentration is of the exponential form. Additionally, it is assumed that the saturation of the N type material ceases at a level of ten times the doping level or about 1.25×10^{15}. The decay can then be expressed as

$$1.25 \times 10^{15} = P_{(9 \times 10^{-2})}\left(1 - e^{-\frac{Y}{0.015}}\right) \qquad (3\text{-}7)$$

and the resistance as

$$R = \frac{Y}{q\mu_n N_D A}\ , \qquad (3\text{-}8)$$

where

$$\mu_n = 1.45 \times 10^3 \text{ and } N_D = 1.25 \times 10^{14}\ . \qquad (3\text{-}9)$$

The values of μ_n and N_D are assumed constant over the radiation levels of concern. The resistance of the unsaturated region R can then be expressed as

$$R = 1005\,\ln\left(1 - \frac{3.88 \times 10^{-6}}{IL_p}\, e^{\frac{0.075}{L_p}}\right)\ . \qquad (3\text{-}10)$$

Under condition of no radiation, a plot of the above equation can be represented as in Figure 6.

The next problem was to determine a model for the saturated resistance; this was accomplished by empirical means. The four unijunction transistors previously referred to were tested on a transistor curve-tracing oscilloscope using the circuit shown in Figure 7.

The dynamic impedance of the transistors was measured at different current levels. These data were averaged and plotted on log-log paper and it was found that a straight line offered the best approximation of these points, as shown in Figure 8. A mathematical expression for the line was found to be

$$\ln R = -0.768\ln I + 0.735\ . \qquad (3\text{-}11)$$

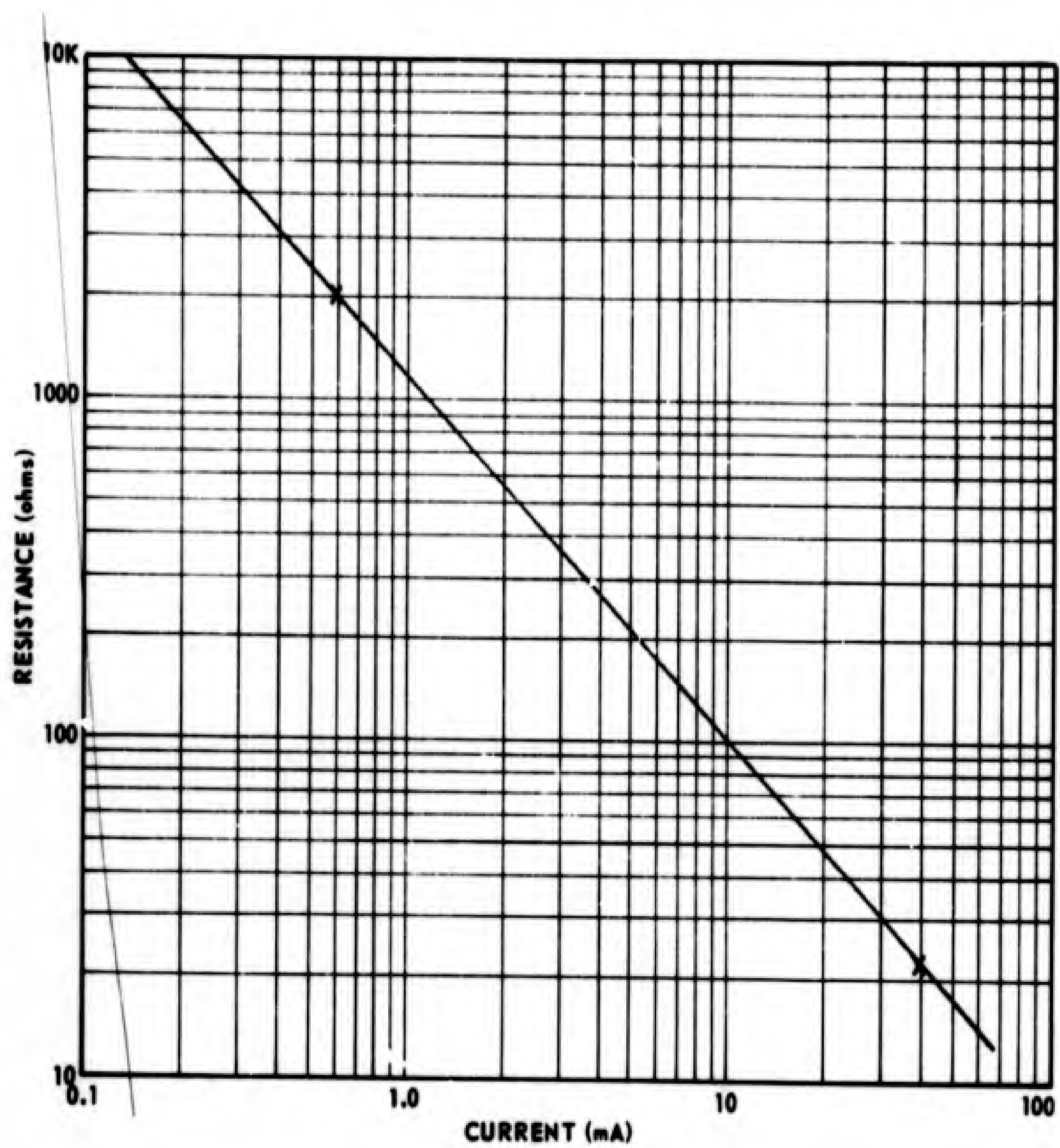

Figure 6. Unsaturated Resistance as a Function of Current for Bar-Type Unijunction

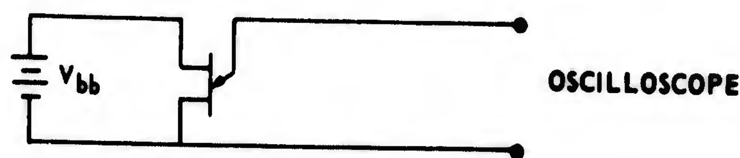

Figure 7. Circuit for Measuring Characteristics Curves

In order to check the conformance of the model with the actual results, the two curves representing the saturated and unsaturated resistance were added to give the composite curve as shown in Figure 9. By combining the composite curve and the network equations, a characteristic curve was calculated and is shown in Figure 10.

The next item to be considered is the radiation effect. The only parameter to be considered as being affected by neutron radiation is the diffusion length L_p. Present literature did not reveal data on the degree of damage that a unijunction would sustain for a specific radiation level. In order to determine the radiation coefficient K for the unijunction, the four 2N491B transistors were irradiated at 1.71×10^{12} neutrons per square centimeter. After irradiation, the characteristics were again measured (Figures 11 through 14).

In order to determine the changes in L_p, the actual results were plotted, and the saturated resistance was subtracted from the main characteristics, leaving the unsaturated resistance. One point was selected to calculate L_p and, therefore, the damage constant. The point selected was 10^{-2} amperes which yielded a resistance of 200 ohms and represented a distance Y of 40×10^{-6} meters. Equations (2-31) and (3-10) can be combined to yield

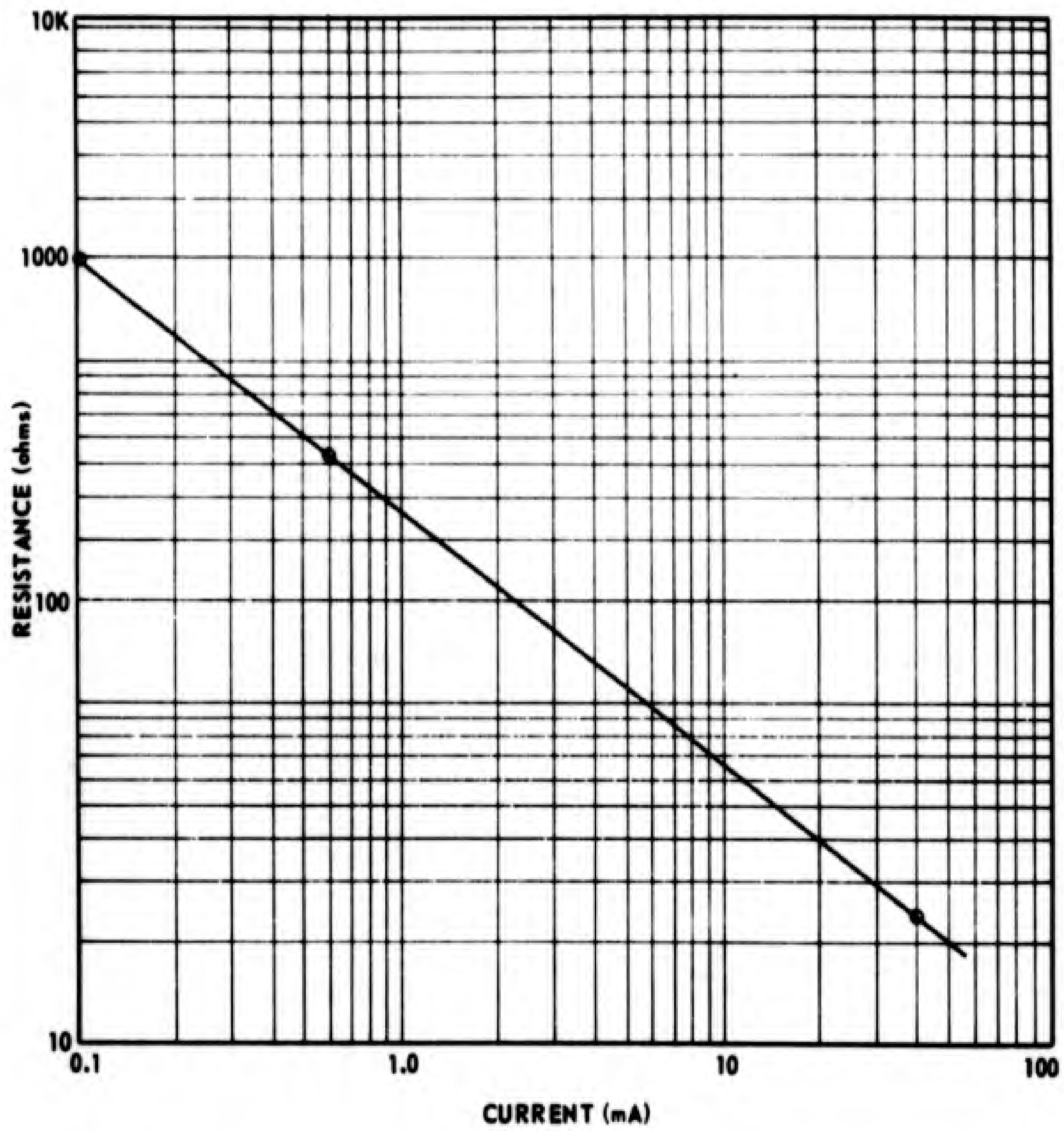

Figure 8. Saturated Resistance as a Function of Current for Bar-Type Unijunction

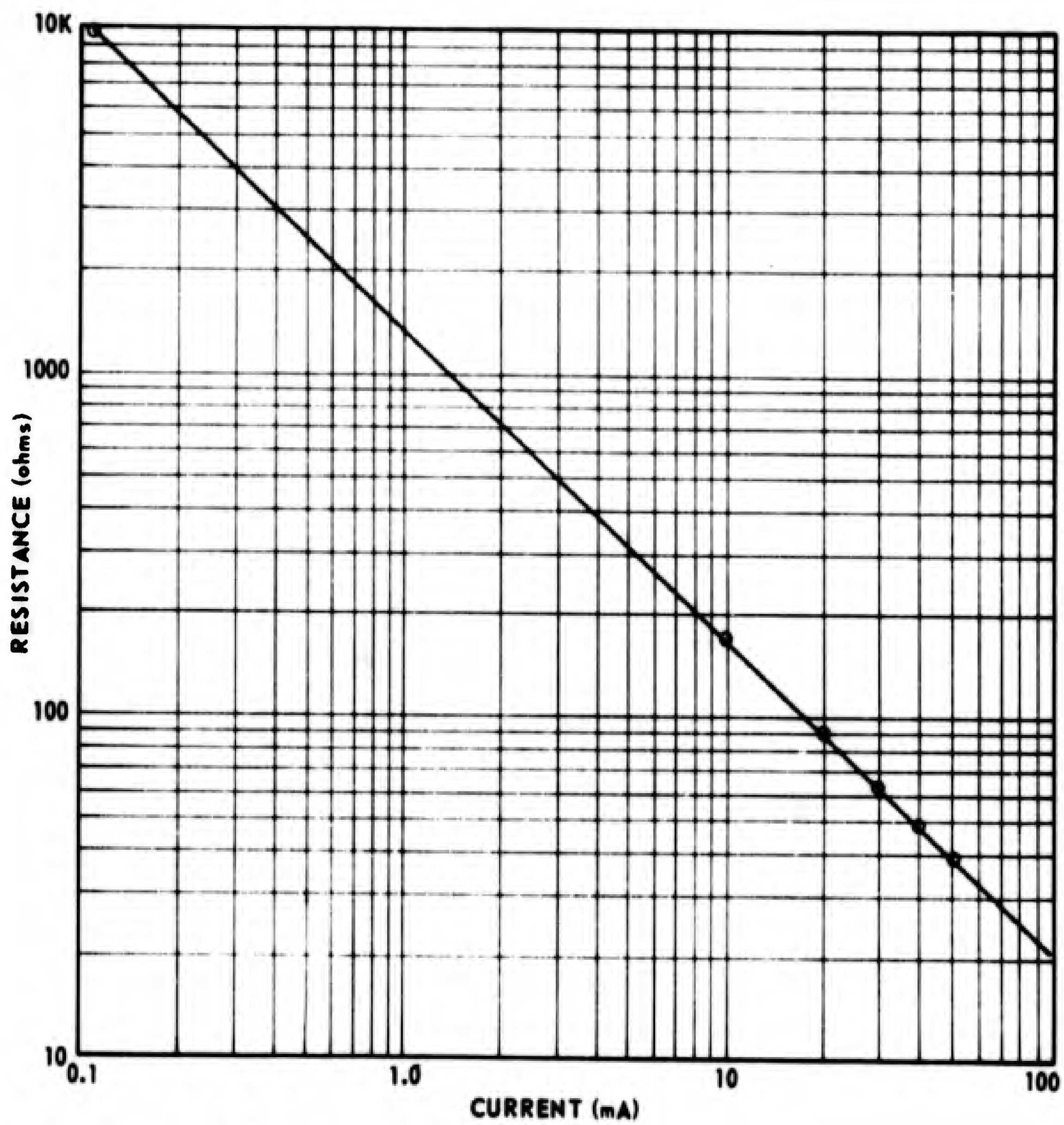

Figure 9. Composite Curve for Bar-Type Unijunction

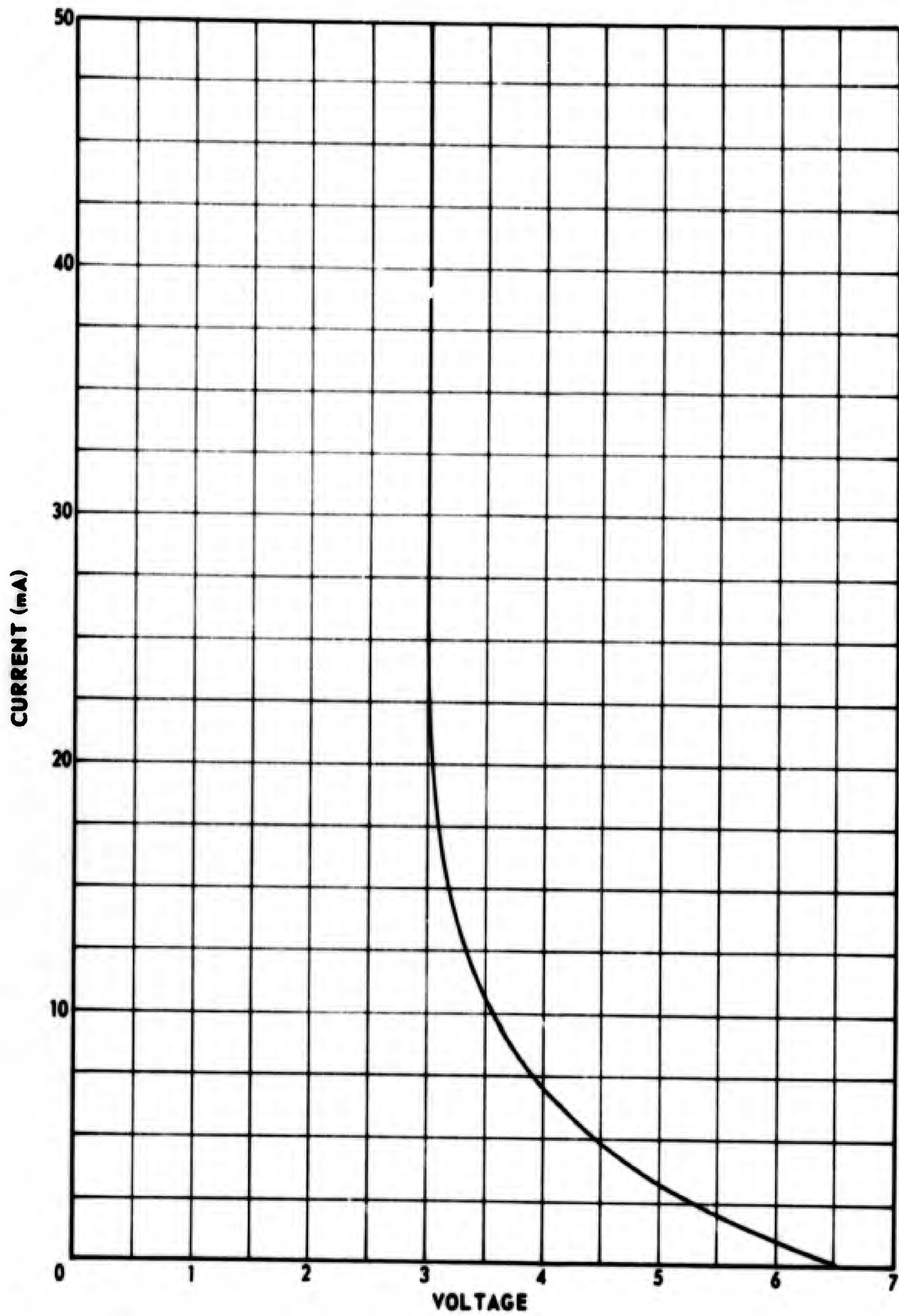

Figure 10. Voltage-Current Characteristic Curve for Bar-Type Unijunction

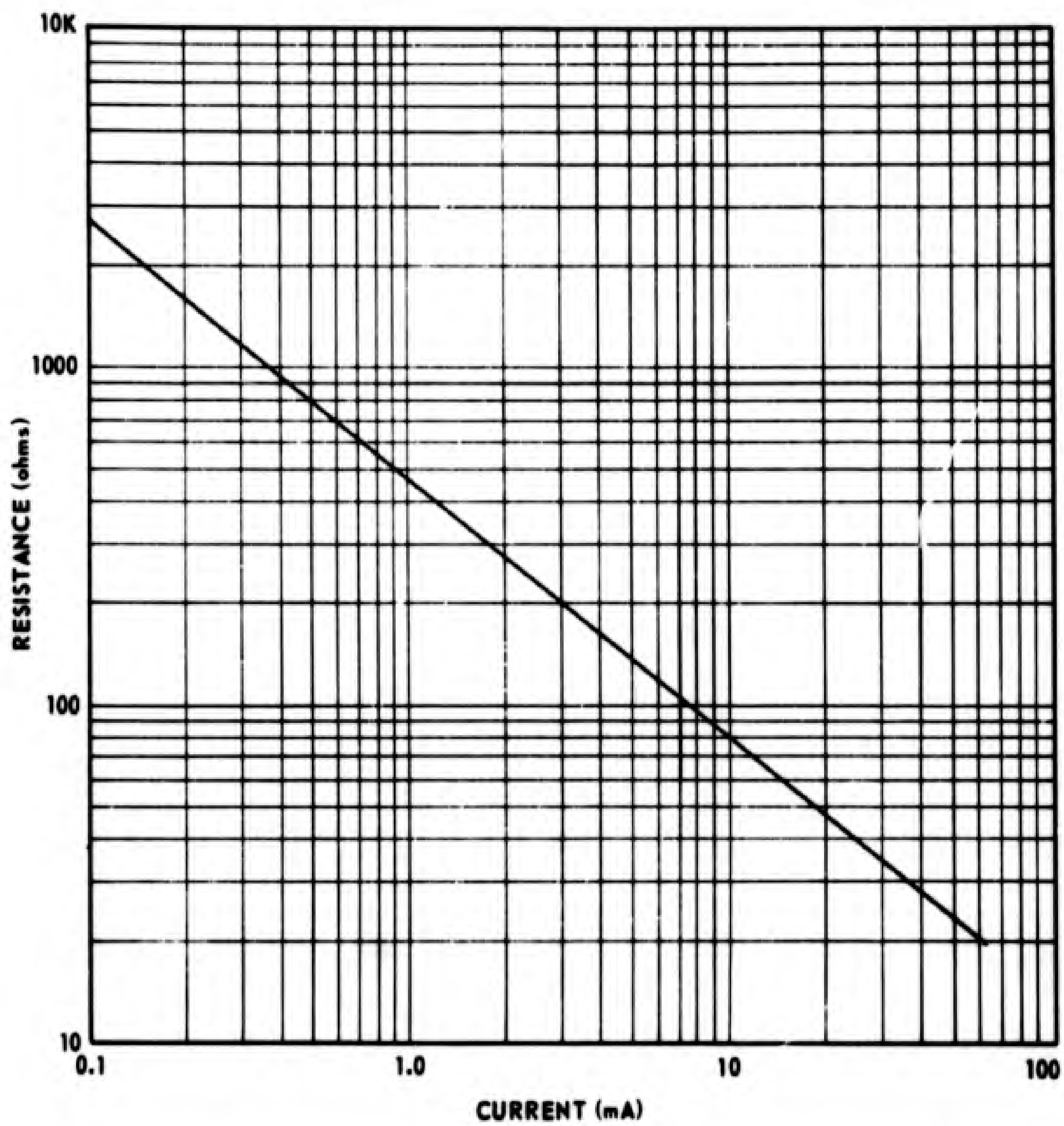

Figure 11. Saturated Resistance for Bar-Type Unijunction
1.71×10^{12} Neutrons per Square Centimeter

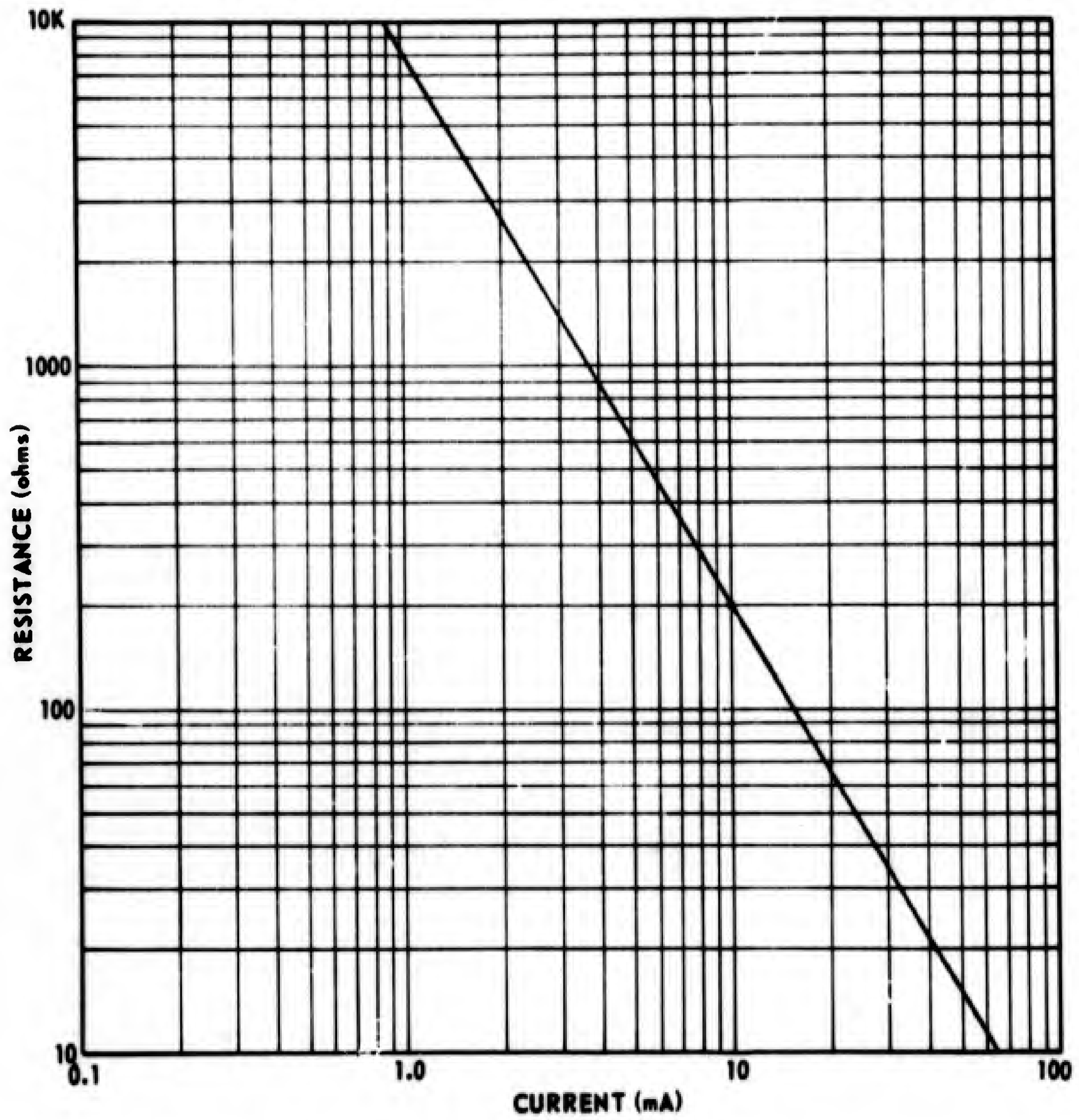

Figure 12. Unsaturated Resistance of Bar-Type Unijunction
1.7×10^{12} Neutrons per Square Centimeter

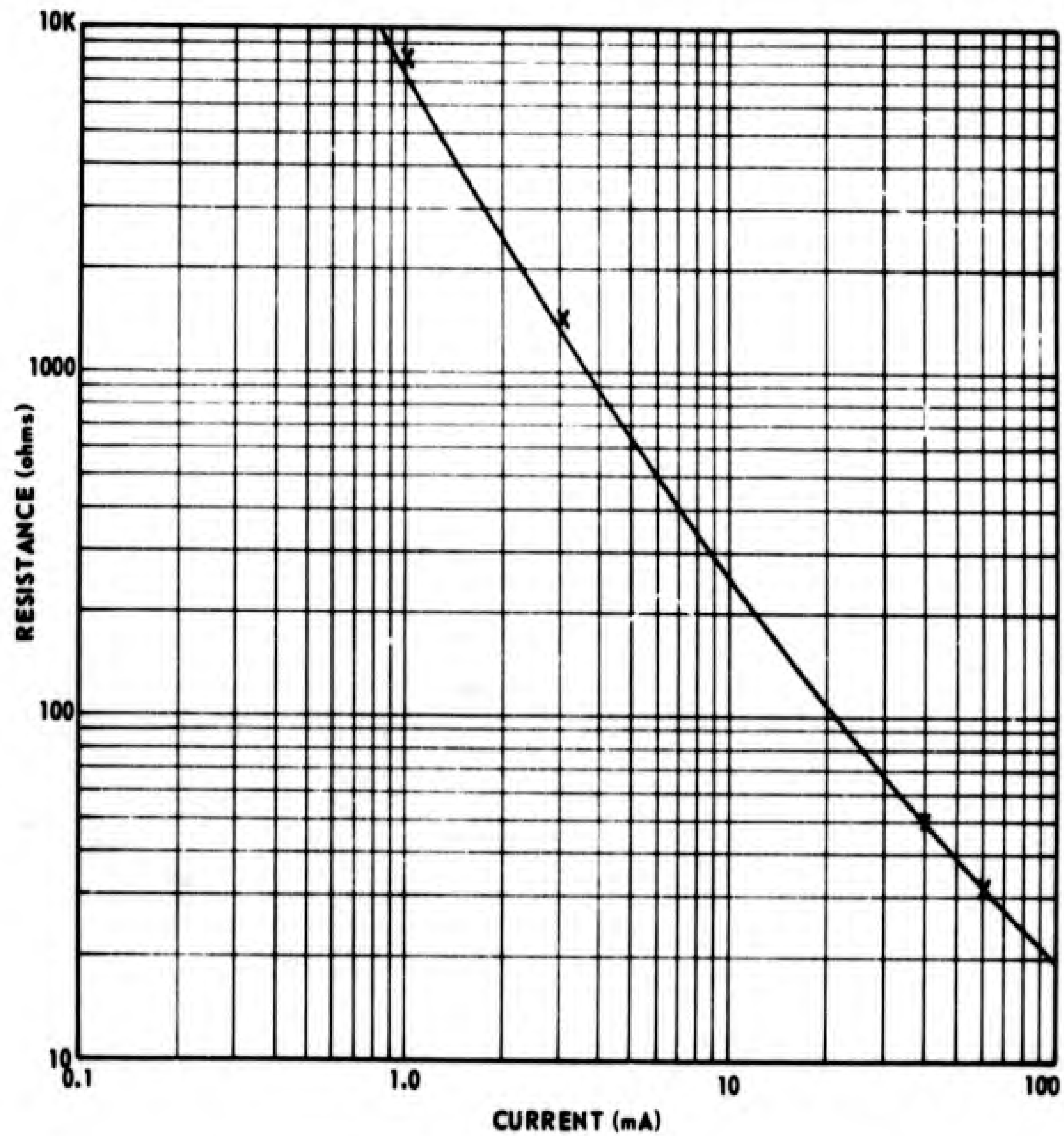

Figure 13. Composite Curve for Bar-Type Unijunction
1.7×10^{12} Neutrons per Square Centimeter

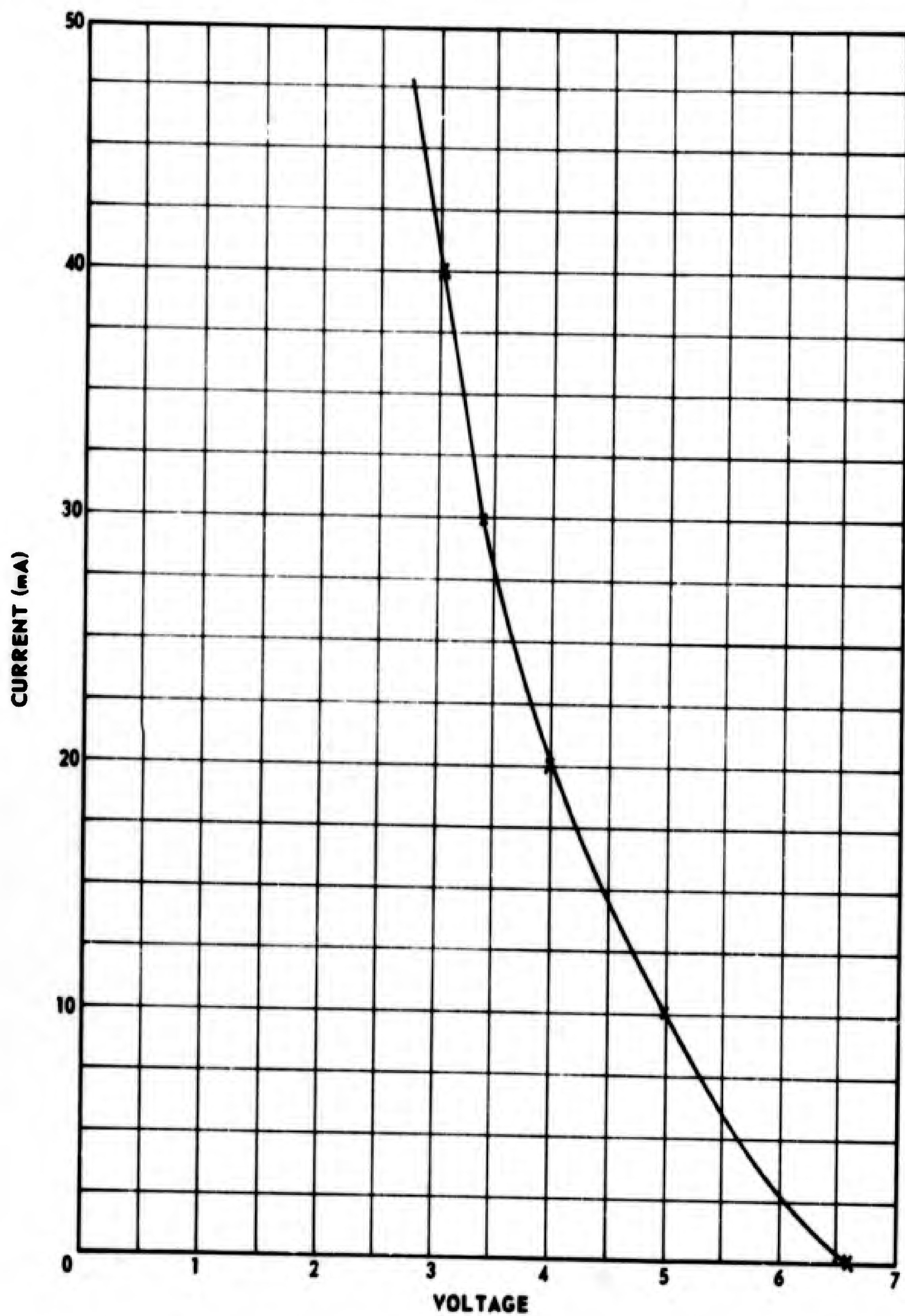

Figure 14. Voltage-Current Characteristic Curve for Bar-Type Unijunction 1.7×10^{12} Neutrons per Square Centimeter

$$0.00215 \ln \left(1 - \frac{3.88 \times 10^{-6} e^{\frac{0.075}{L_p}}}{0.01 L_p}\right) = 0.004 \qquad (3\text{-}12)$$

$$L_p = 0.0198 \text{ cm} \ .$$

It has been established that the diffusion length L_p changed from 0.036 centimeter with no radiation to 0.0198 centimeter with 1.71×10^{12} neutrons per square centimeter. A knowledge of this change then permits a calculation of the damage coefficient K.

$$L_p = \left(\tau D_n\right)^{1/2} \qquad (3\text{-}13)$$

$$\frac{1}{\tau} = \frac{1}{\tau_o} + K\phi \ . \qquad (3\text{-}14)$$

Then

$$K = 1.30 \times 10^{-8} \ .$$

The next problem was to develop the expression for the radiation effect on the saturation resistance. The unirradiated expression for the saturation resistance was found by using the general equation for a line and is given as

$$\ln R = -0.768 \ln I + 0.735 \ . \qquad (3\text{-}15)$$

The case for 1.71×10^{12} neutrons per square centimeter was found to give

$$\ln R = -0.72 \ln I + 1.3 \ . \qquad (3\text{-}16)$$

Utilizing the general form of equations (3-15) and (3-16) and knowing that they are a function of diffusion length, the author predicts the following empirical relation:

$$R = \frac{e^{\frac{0.0264}{L_p}}}{I\left(0.657 + 3.09L_p\right)} \quad . \qquad (3\text{-}17)$$

If the diode junction voltage is assumed to be 0.6 volts, the transistor operating characteristic at given radiation levels can be predicted. Because the values of radiation doses on the actual test units were 1.73×10^{12} and 7.29×10^{12} neutrons per square centimeter, these values were used in the prediction. From equation (3-14), the diffusion length L_p becomes 0.0036 centimeter at 7.29×10^{12} neutrons per square centimeter.

Unijunction failure was defined to exist when a current of 10^{-2} amperes fails to hold the unijunction in the on state. Such failure occurred at a diffusion length of 0.0195 centimeter. The corresponding level of radiation when failure occurred can be determined as follows

$$(0.0195)^2 = 13\tau$$

$$\tau = 2.9 \times 10^{-5}$$

$$\frac{1}{\tau} = \frac{1}{\tau_o} + K\phi$$

$$\tau_o = 10^{-4}$$

$$K = 1.30 \times 10^{-8}$$

$$\phi = 1.93 \times 10^{12}\ n/cm^2 \approx 2 \times 10^{12}\ n/cm^2 \ .$$

When the predicted characteristics are compared with the actual oscilloscope traces shown in Chapter IV, it is apparent that the 2N3980 and 2N3480 units do not conform to this predicted technique. The reason for this

discrepancy is due to construction of these devices. The construction of these units was found to be monolithic compared with the bar-type in the 2N491B unit. One of the 2N3980 unijunction transistors was opened and the semi-conductor chip removed. This chip was measured under a comparison micro-scope, and a drawing of the semiconducting chip with the measured dimensions is shown in Figure 15.

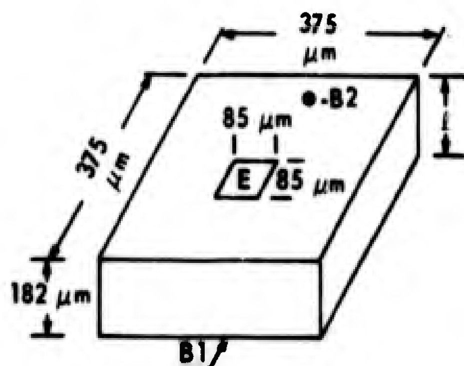

Figure 15. Monolithic-Type Construction

The doping levels and resistivity were obtained from the manufacturer and were found to be identical with the bar-type previously discussed. The resis-tance between B1 and B2 was measured and found to be 3.9 kilohms. The effective area can be calculated by

$$R = \frac{\rho \ell}{A} = \frac{\ell}{A q \mu_n N_p} .$$

The effective area was used instead of the actual measured area because the electric field is forced into a nonuniform geometry between the contacts B1 and B2.

An equivalent model of the monolithic unijunction is shown in Figure 16.

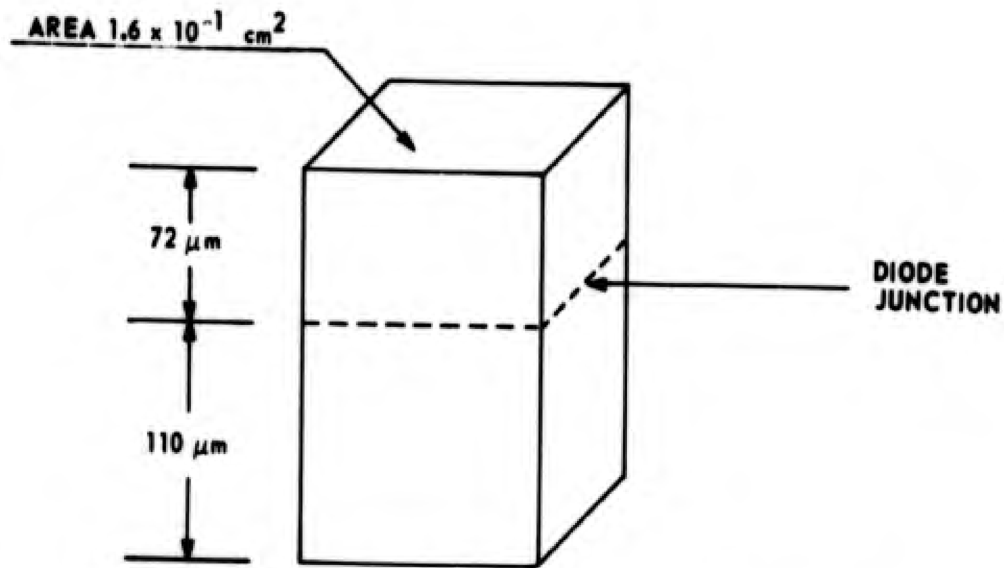

Figure 16. Effective Model of Monolithic Unijunction

This model allows the use of the previously derived expression for the bar-type. All factors should remain the same except for a change in ℓ. It should be noted here that the monolithic unijunction is operated in a condition where L_p is long in comparison with the diffusion length.

$$\rho_{(\ell)} = \Delta P_{(0)} e^{\frac{\ell}{1.2L_p}}$$

$$\rho_{(\ell)} = \Delta P_{(0)} e^{\frac{0.00916}{L_p}}$$

$$\rho_{(\ell)} = \frac{IL_p}{3.1 \times 10^{-21}} e^{\frac{0.0916}{L_p}} ,$$

where

$$\ell = 110 \times 10^{-4} \text{ m} .$$

By applying equations (3-7) and (3-10), the following relations can be expressed

$$1.25 \times 10^{15} = \rho_{(\ell)} \left(1 - e^{-\frac{Y}{0.0215}} \right)$$

$$R = 465 \, \mathcal{L}n \left(1 - \frac{3.88 \times 10^{-6}}{IL_p} e^{\frac{0.00916}{L_p}} \right) .$$

The saturation resistance was measured and added to the unsaturated resistance. A very interesting change occurs in the characteristic of the device and is attributed to the construction of the device. With large currents being driven into the junction, the unsaturated resistance essentially becomes constant with increased current. The characteristics obtained for this unsaturated resistance are shown in Figure 17.

The next step is to compare the prediction technique with the irradiated case 7.36×10^{12} neutrons per square centimeter. The damage constant ($K = 1.3 \times 10^{-8}$ cm^2/n-sec) is assumed to remain the same. Thus the diffusion length is reduced to 0.0112 centimeter which is the approximate length of material.

By adding the predicted saturated resistance to the predicted unsaturated resistance, a composite curve is obtained and from this composite curve the voltage-current characteristic curves can be determined (Figures 18 and 20).

No appreciable change in saturated resistance was noted over the range of neutron fluence.

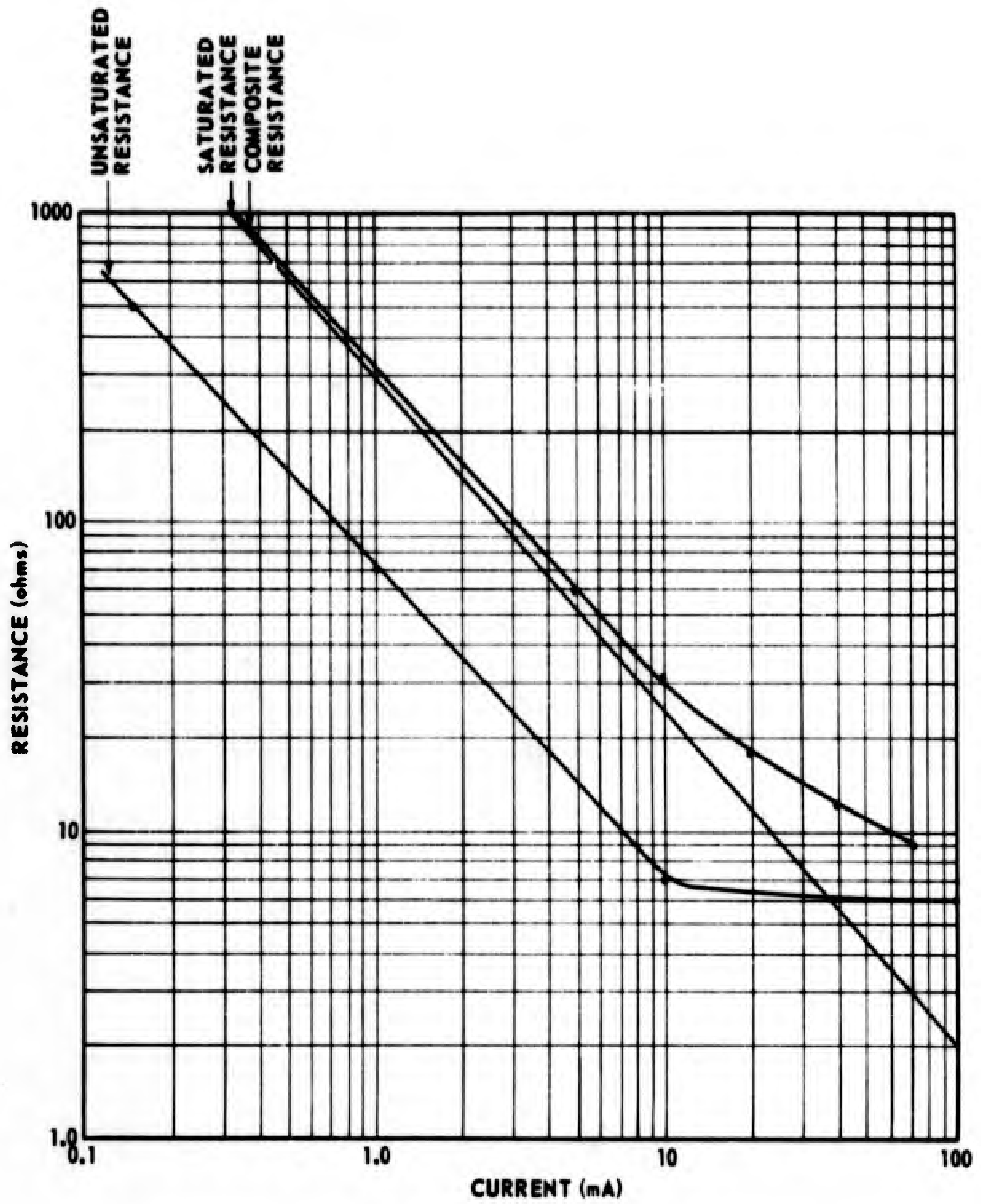

Figure 17. Characteristic Curve for Monolithic-Type Unijunction

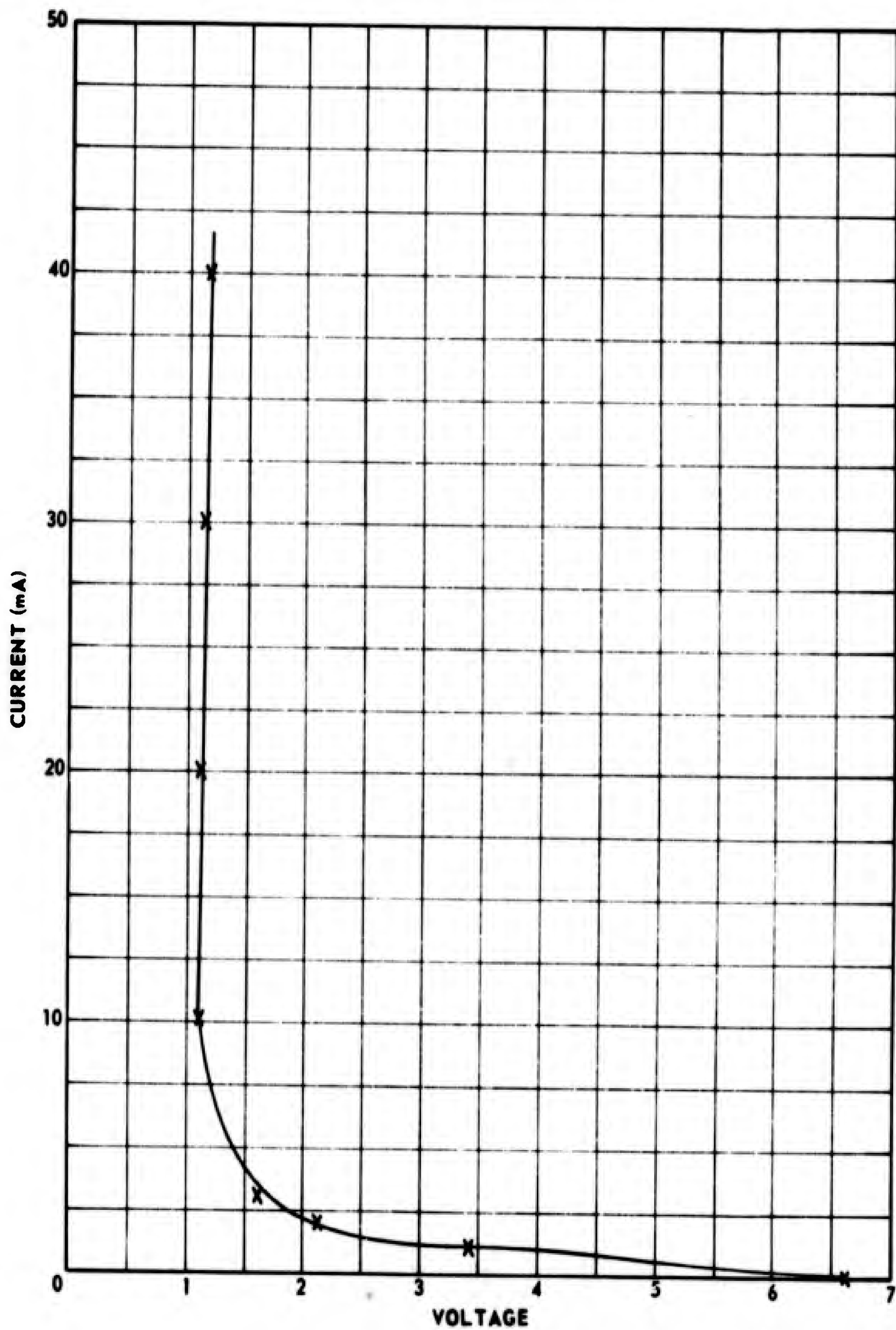

Figure 18. Voltage-Current Characteristic Curve for Monolithic-Type Unijunction

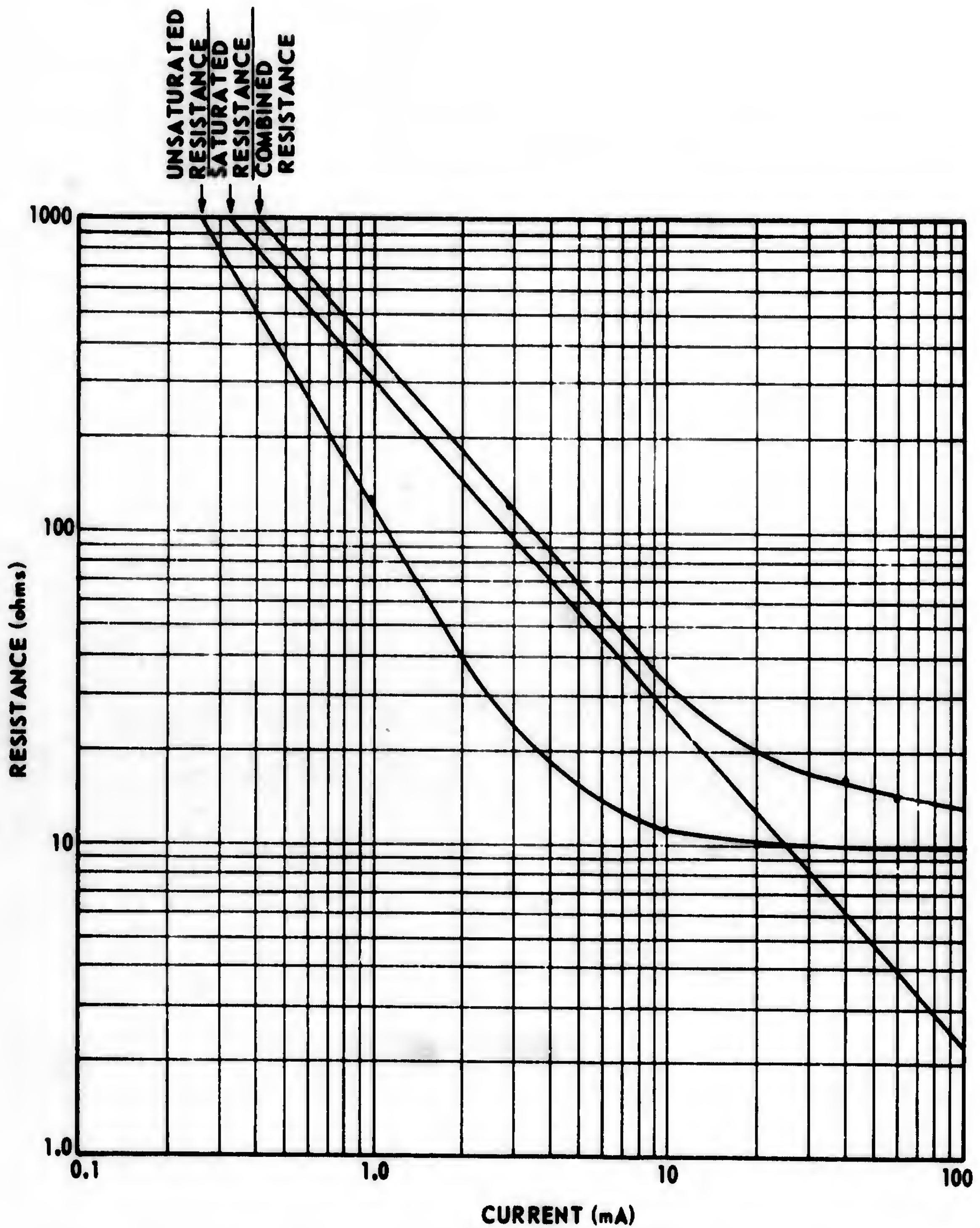

Figure 19. Characteristic Curve for Monolithic-Type Unijunction 7.3×10^{12} Neutrons per Square Centimeter

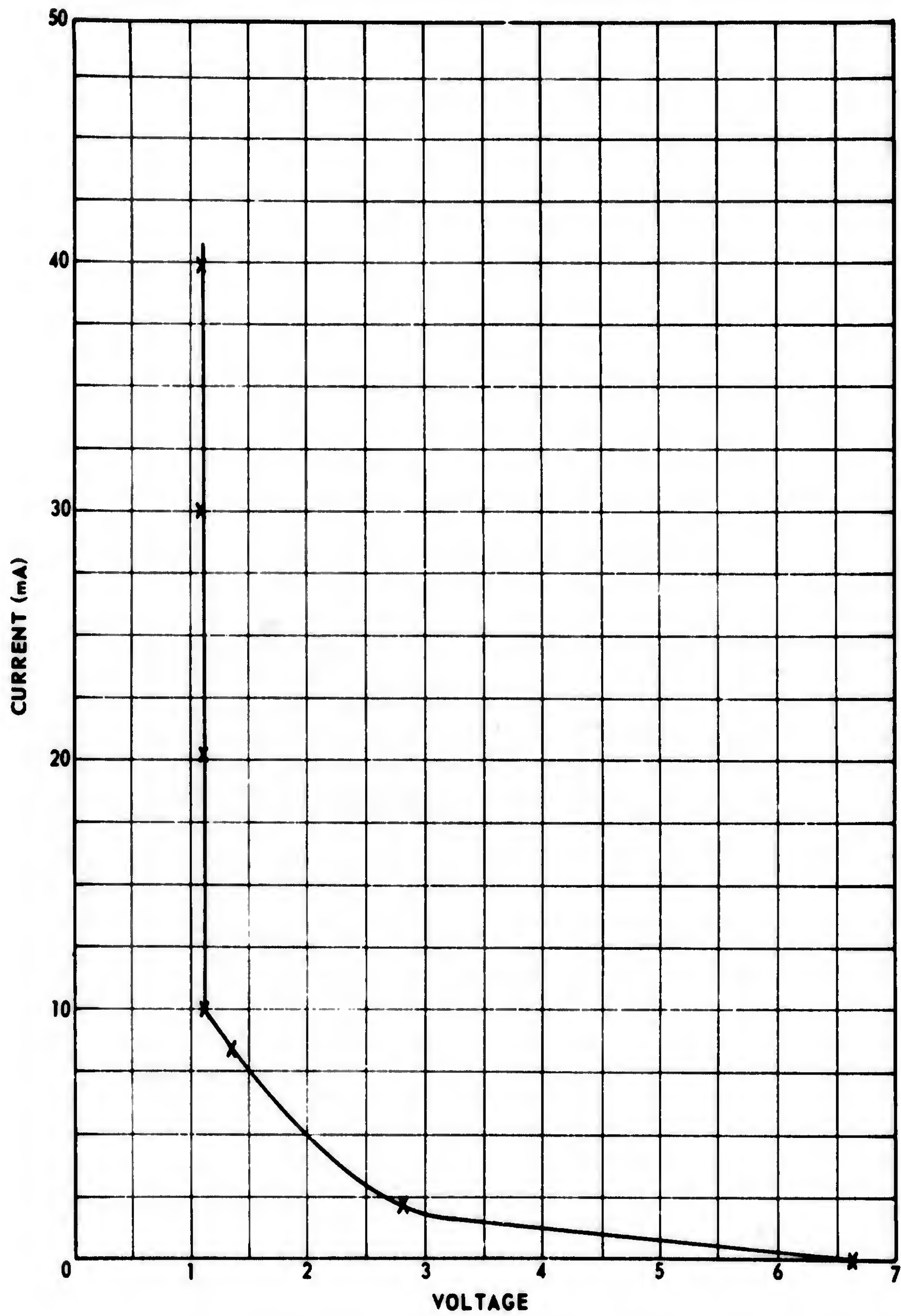

Figure 20. Voltage-Current Characteristic Curve for Monolithic-Type Unijunction 7.3×10^{12} Neutrons per Square Centimeter

B. Silicon Control Rectifier Damage

The silicon control rectifier is composed of alternate layers of P and N types of materials. This four-layer device can be modeled with two transistors, one being an N-P-N transistor and the other being a P-N-P transistor. The base of the P-N-P transistor is connected to the collector of the N-P-N transistor and the collector of the P-N-P transistor tied to the N-P-N transistor's base. This connection forms the gate. This device is bistable. That is, it is either in saturation or is off. When both transistors are in the off mode, a high resistance is developed between the emitters of the tow transistors. When the gate current is sufficiently high to allow the product of the two gains to be equal to unity, the device goes into saturation. Once the device is in saturation, it remains saturated until power is removed. This is due to regeneration between the two transistors in this equivalent circuit.

The SCR's gain H_{fe} is a function of neutron fluence, and when the gain-bandwidth-product falls below one for any current level the SCR will not saturate. Calculation of this level of radiation can be accomplished in the following manner. Consider that the base region of the P-N-P transistor is 75×10^{-6} meters and the base region of the N-P-N transistor is 30×10^{-6} meters. In order to find the radiation level, the base transient time can be found from the following equation [13]

$$t_{bp} = \frac{W^2}{b}\left(\frac{m - 1 + e^{-m}}{m^2}\right), \qquad (3\text{-}18)$$

where

$$D_p = 15 \ ,$$

$$m = \mathcal{L}n\left(\frac{N_e}{N_o}\right),$$

$$N_e = 5 \times 10^{18}/\text{cm}^3 \ ,$$

and

$$N_o = 10^{11}/\text{cm}^3 \ .$$

By proper substitution of these values into equation (3-18), t_{bp} can be found and is given as $t_{bp} = 55$ n-sec. However, t_{bp} is not the major contributor to the radiation damage. The low-doped N region is in high injection and base transit time can thus be expressed as

$$t_{bn} = \frac{1}{2}\left(\frac{W^2}{2b}\right) \qquad (3\text{-}19)$$

where

$$b = 13 \ .$$

Then

$$t_{bn} = 1.08 \ \mu\text{sec} \ .$$

The minimum criterion for turn-on is expressed as

$$\left(\frac{1}{H_{fen}}\right)\left(\frac{1}{H_{fep}}\right) = 1 \ , \qquad (3\text{-}20)$$

where

$$\frac{1}{H_{fen}} \approx t_{bn} K\phi \ ,$$

and

$$\frac{1}{H_{fep}} \approx t_{bp} K \phi \ .$$

By expressing the elements in equation (3-20) in terms of their approximate equivalences related to base transistor time, the radiation fluence can be expressed as follows

$$\phi = \frac{1}{K}\left(\frac{1}{t_{bp} t_{bn}}\right)^{1/2} \ . \qquad (3\text{-}21)$$

The constant K has a value of 10^6 $cm^2/n\text{-}sec$; therefore

$$\phi = 4 \times 10^{12} \ n/cm^2$$

CHAPTER IV

PROCEDURE AND RESULTS OF RADIATION TEST

A. Irradiating Procedure

Twenty-four unijunction transistors and nine silicon control rectifiers were mounted on a sheet of styrofoam in the retainer pattern shown in Figure 21.

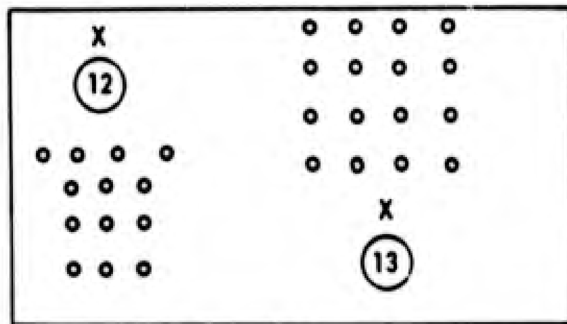

Figure 21. Mounting Configuration

The X 's indicate the location of the dosimeters. This assembly was taken to the White Sands Missile Test Range fast burst reactor and irradiated. The irradiation levels as indicated by the two dosimeters are expressed in Table I. The dose received by each dosimeter can be seen in Table I.

Table I. Irradiation Levels

Dosimeter	Shot	Dosimeter Measurement (n/cm^2)	Average Level (n/cm^2)	Dose Total (n/cm^2)
12	1	5.7×10^{11}		
13	1	5.7×10^{11}	5.7×10^{11}	5.7×10^{11}
12	2	1.17×10^{12}		
13	2	1.15×10^{12}	1.16×10^{12}	1.73×10^{12}
12	3	5.71×10^{12}		
13	3	5.6×10^{12}	5.56×10^{12}	7.29×10^{12}

Between each shot the transistors and SCR's were removed and their characteristics checked. The characteristics were measured on a transistor curve tracing scope (Tektronix model 575), and are shown in Figures 22 through 30.

B. Results

After the comparison of the predicted characteristic, Figure 9, with the characteristics of the actual units, Figures 22 through 30, it is apparent that a discrepancy exists. This difference is about 20 ohms in the monolithic case and about 40 ohms in the bar-type.* These differences do not appear to be affected by neutron radiation.

---

* These resistances are attributed to the ohmic contact which were originally considered to be in the range of milliohms.

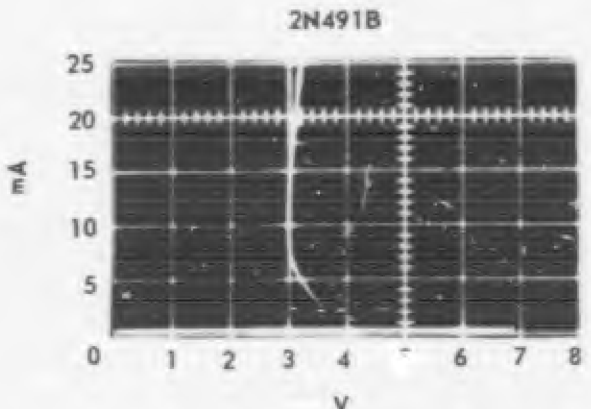

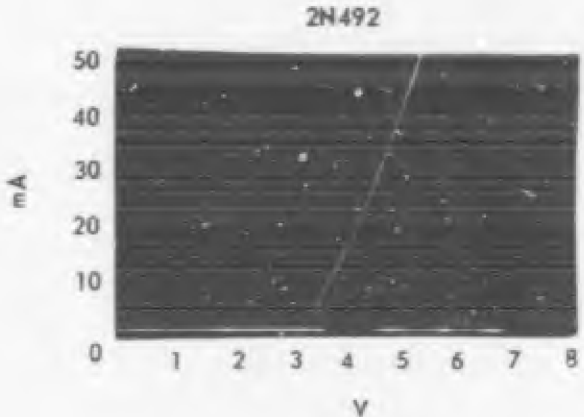

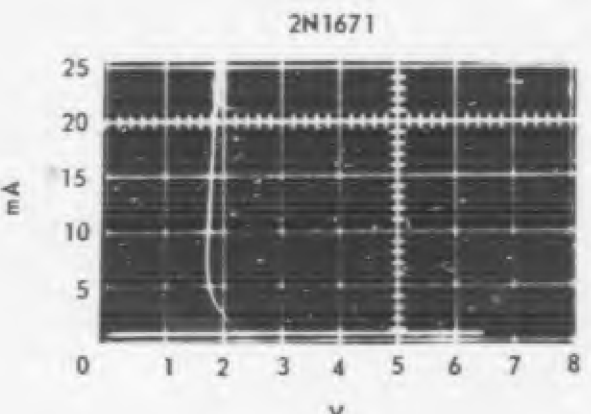

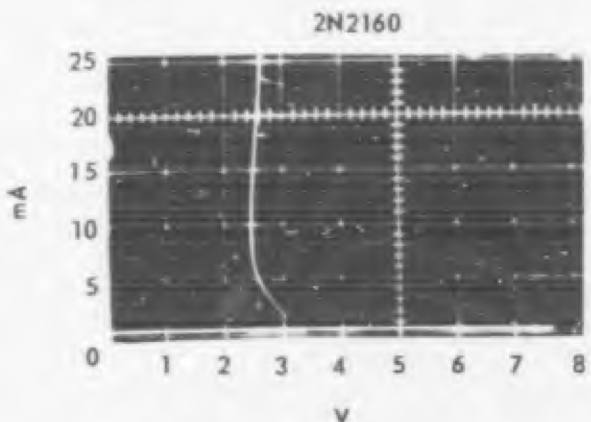

Figure 22. Bar-Type Unijunction Without Radiation

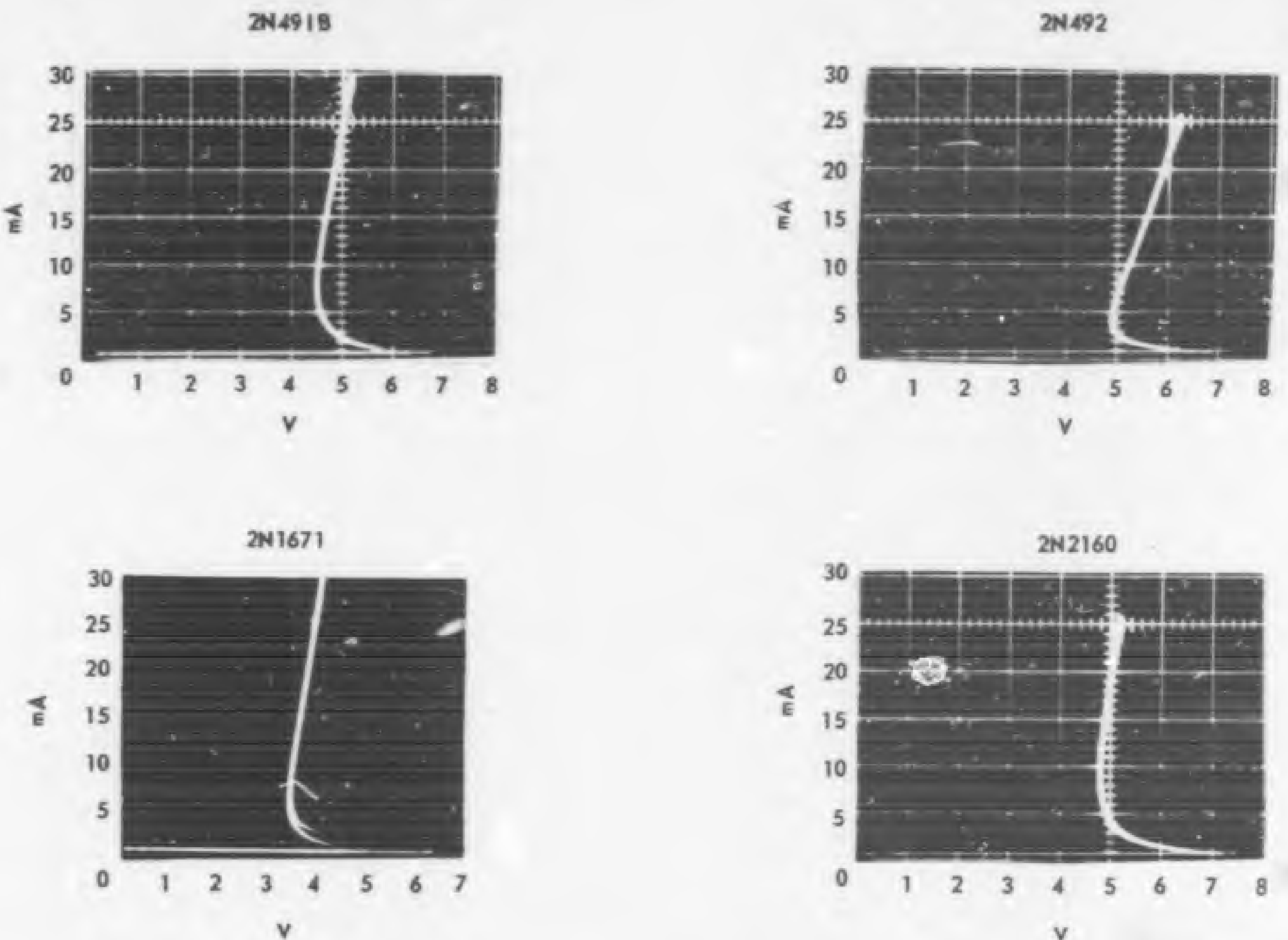

Figure 23. Bar-Type Unijunction with 1.7×10^{12} Neutrons per Square Centimeter

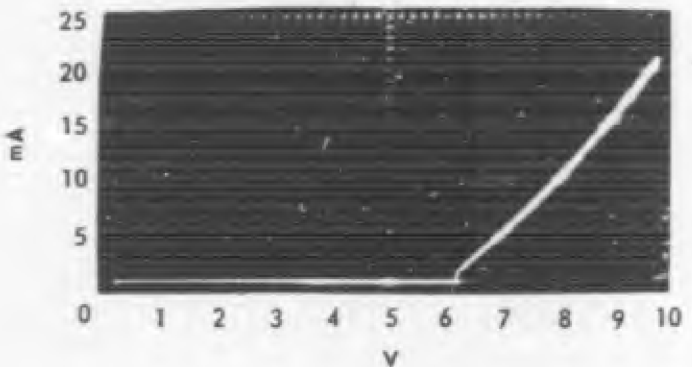

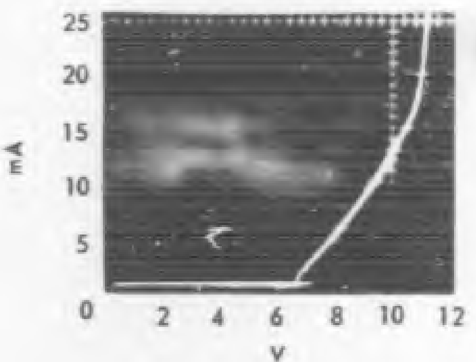

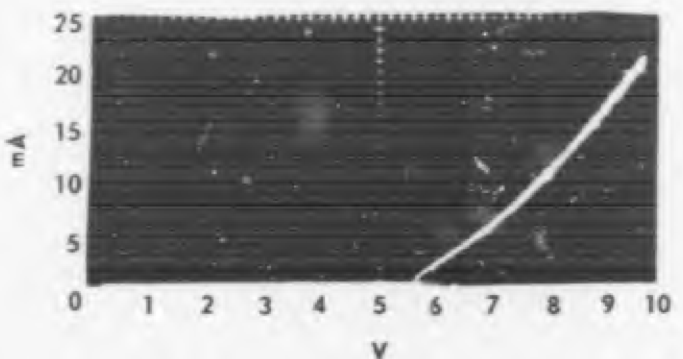

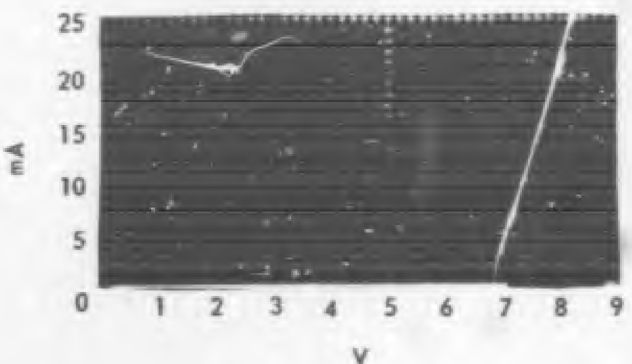

Figure 24. Bar-Type Unijunction with 7.3×10^{12} Neutrons per Square Centimeter

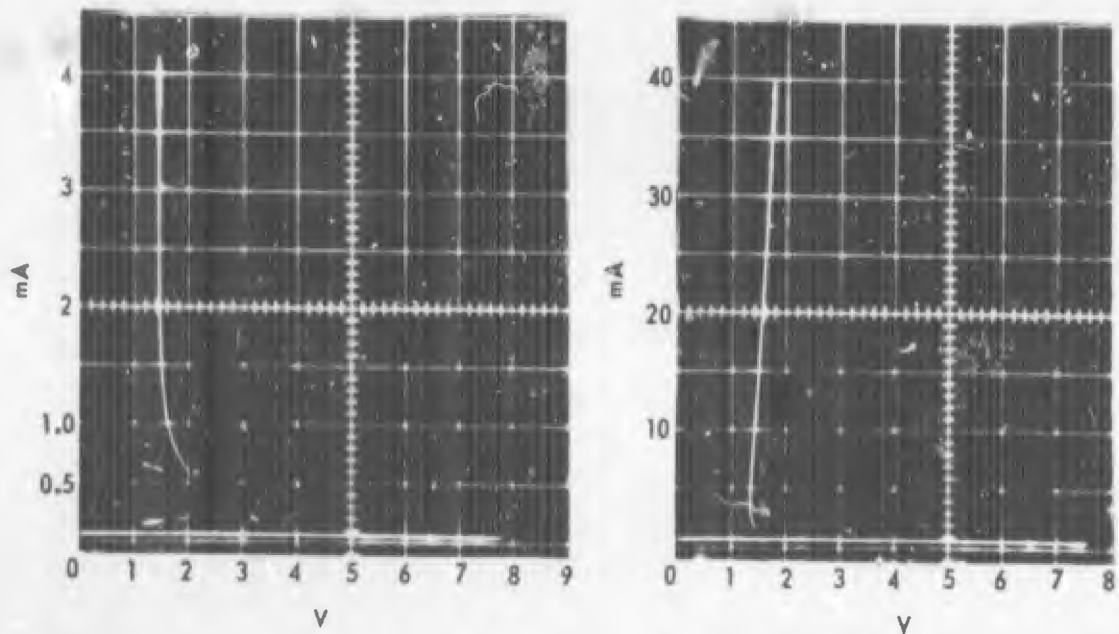

Figure 25. 2N3980 Voltage-Current Characteristics for No Radiation

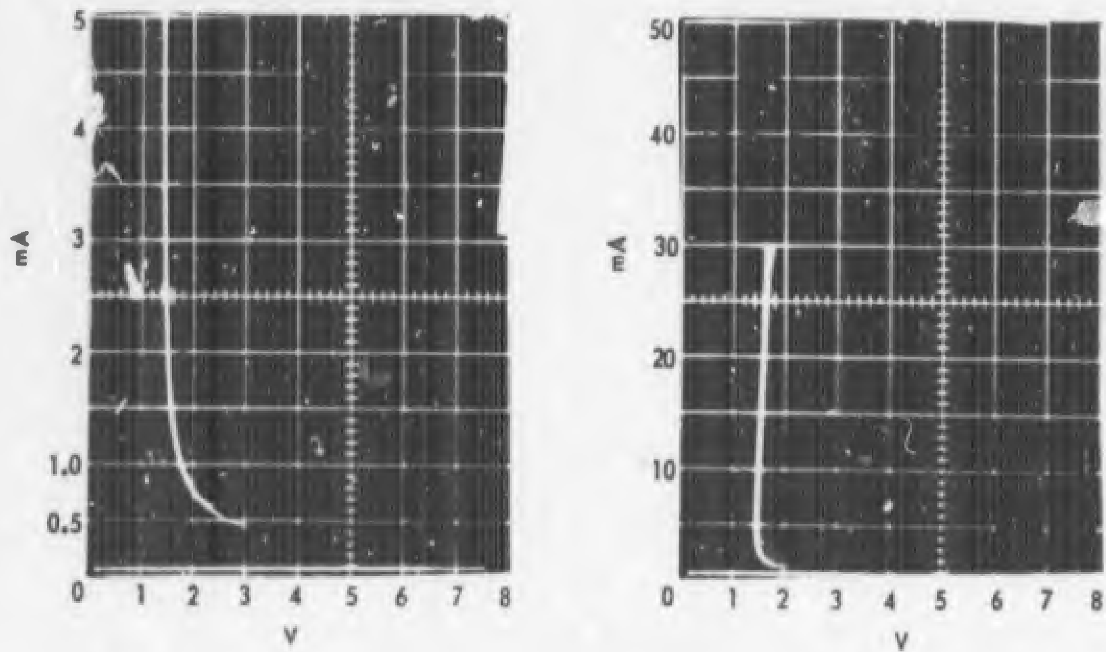

Figure 26. 2N3980 Voltage-Current Characteristics for 1.73×10^{12} Neutrons per Square Centimeter

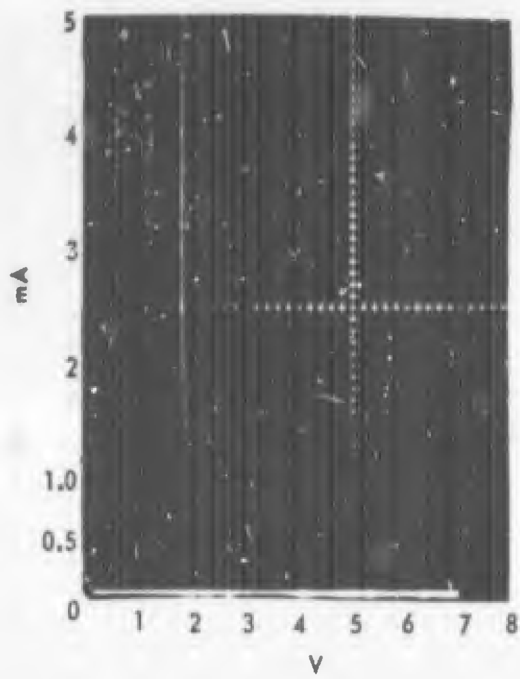

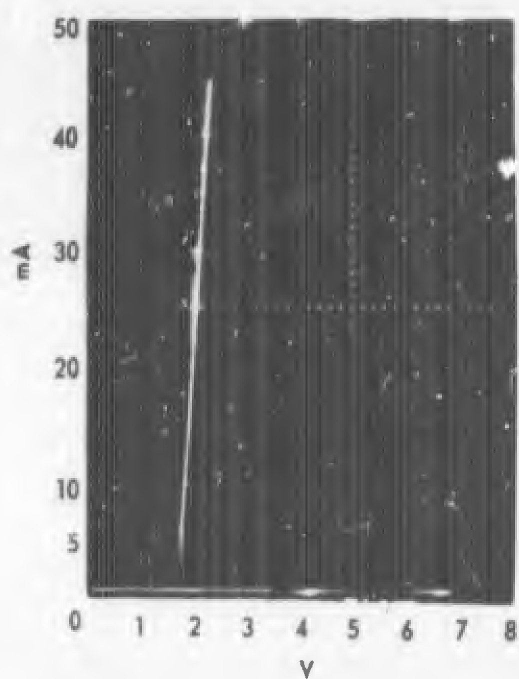

Figure 27. 2N3980 Voltage-Current Characteristics for 7.3×10^{12} Neutrons per Square Centimeter

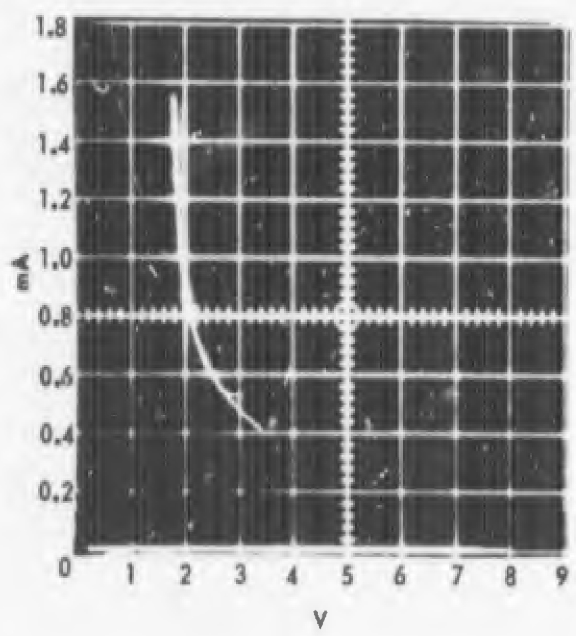

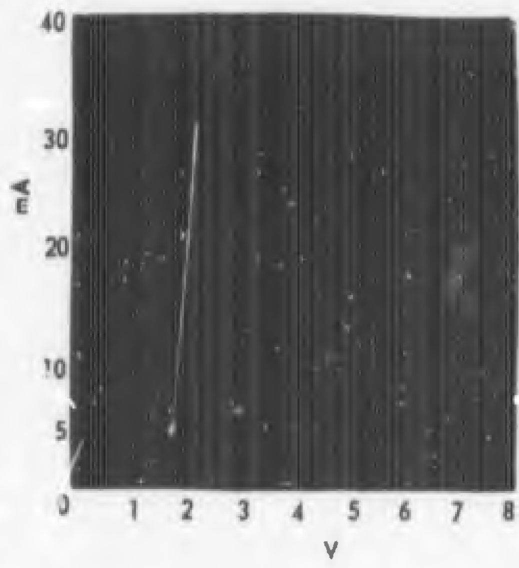

Figure 28. 2N3480 Voltage-Current Characteristics for No Radiation

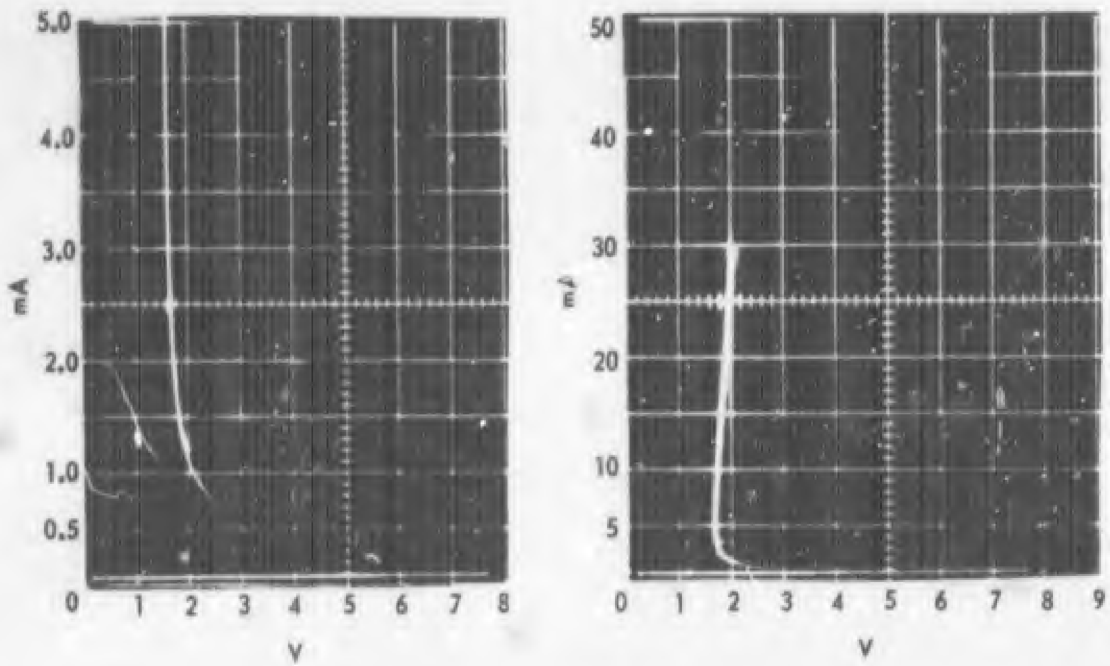

Figure 29. 2N3480 Voltage-Current Characteristics for 1.7×10^{12} Neutrons per Square Centimeter

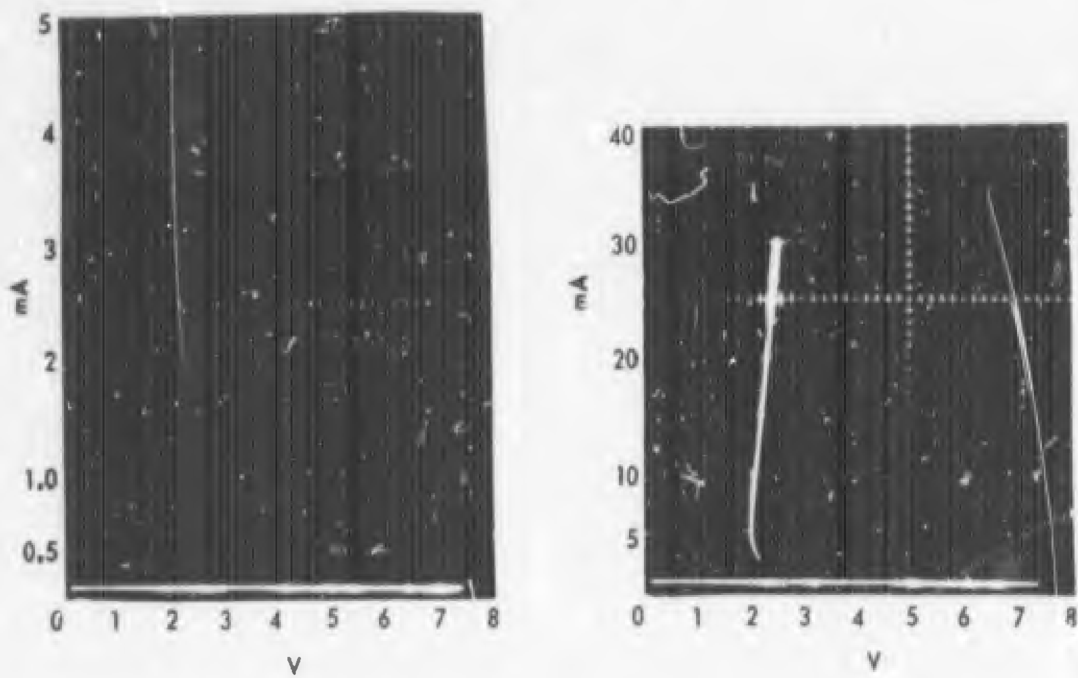

Figure 30. 2N3480 Voltage-Current Characteristics for 7.3×10^{12} Neutrons per Square Centimeter

The network model can now be modified as shown in Figure 31.

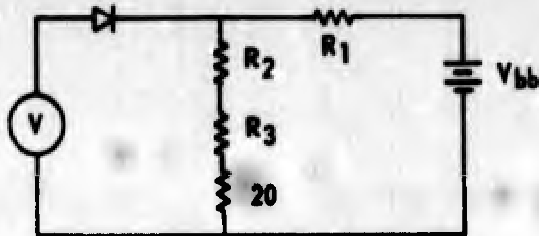

Figure 31. Modified Equivalent Circuit

The 20 ohms is added to the prediction curves in Figures 8, 13, 17, and 19. The revised resistance-current curves are shown in Figures 32,34, 36, and 38. From these revised resistance-current curves are obtained voltage-current curves which are shown in Figures 33, 35, 37, and 39. By adding this correction resistance, the calculated voltage-current characteristic curves compare favorably with the scope photographs.

Three SCR's of four units each were irradiated. The initial characteristics that were measured were firing current, length of firing current, and saturation voltage. The 2N1772 SCR was used as the test case. All units were irradiated, and the results are shown in Figures 40 through 42. The firing current characteristics of the 2N1595 were statistically reduced to one curve, and this curve was used to generate a prediction curve shown in Figure 43. SCR firing current characteristic is plotted on the same graph as its prediction curve. An increase in the length of firing current to 2 n-sec was noted for fluence of 10^{12} neutrons per square centimeter. A theory explaining this change has not been developed, but this change in time should be taken into consideration.

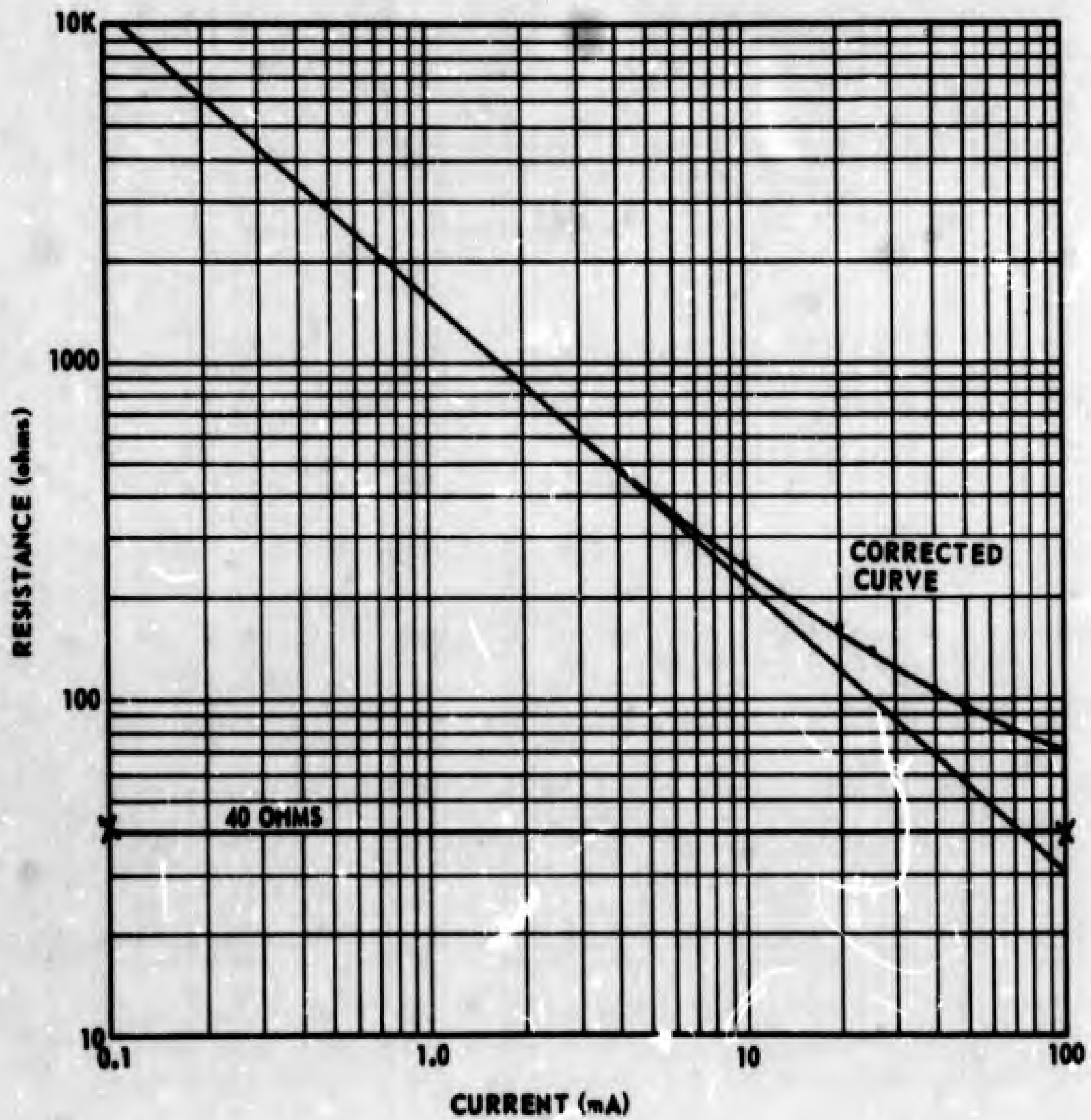

Figure 32. Corrected Characteristic Curve for Bar-Type Unijunction

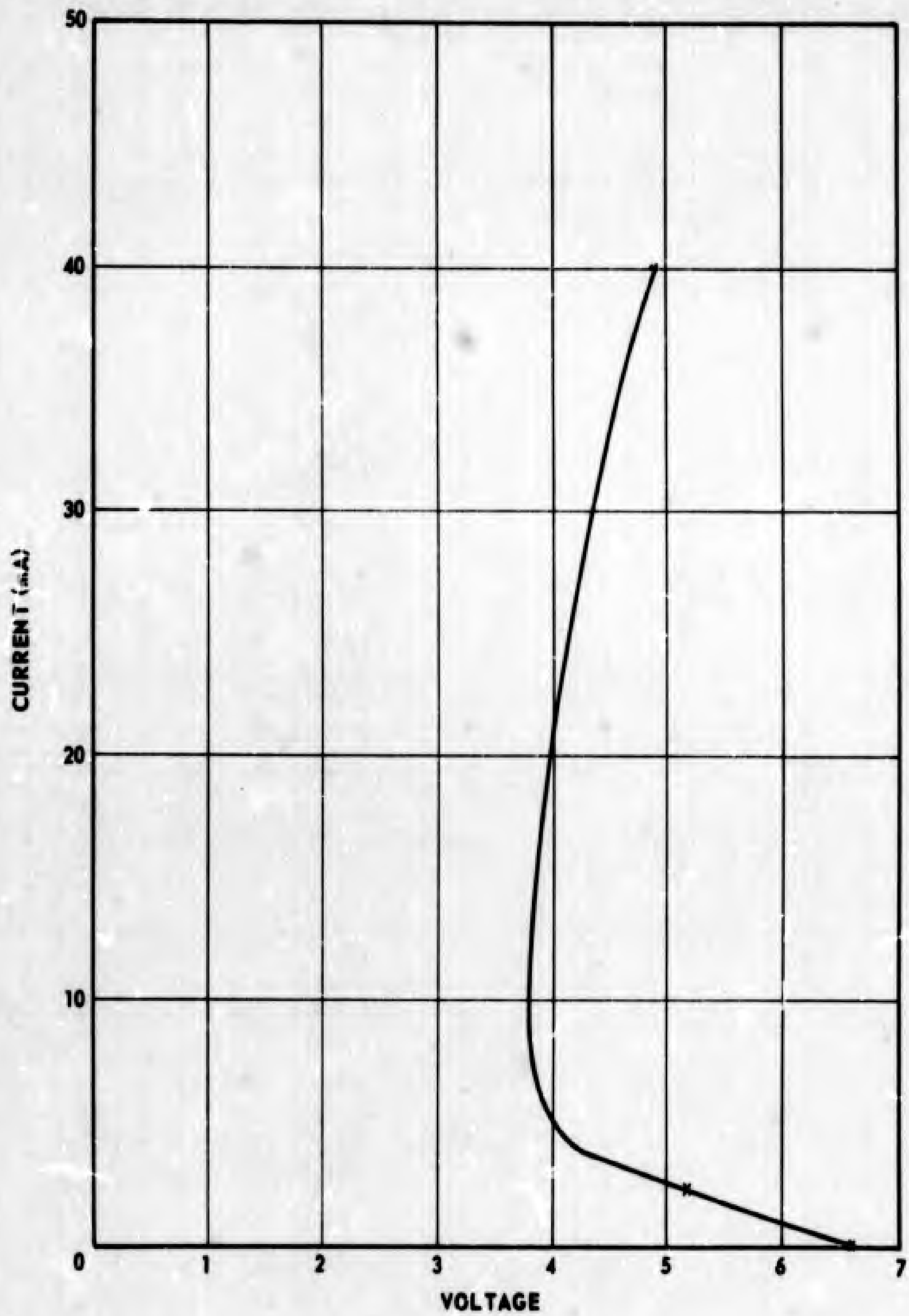

Figure 33. Corrected Voltage-Current Characteristic Curve for Bar-Type Unijunction

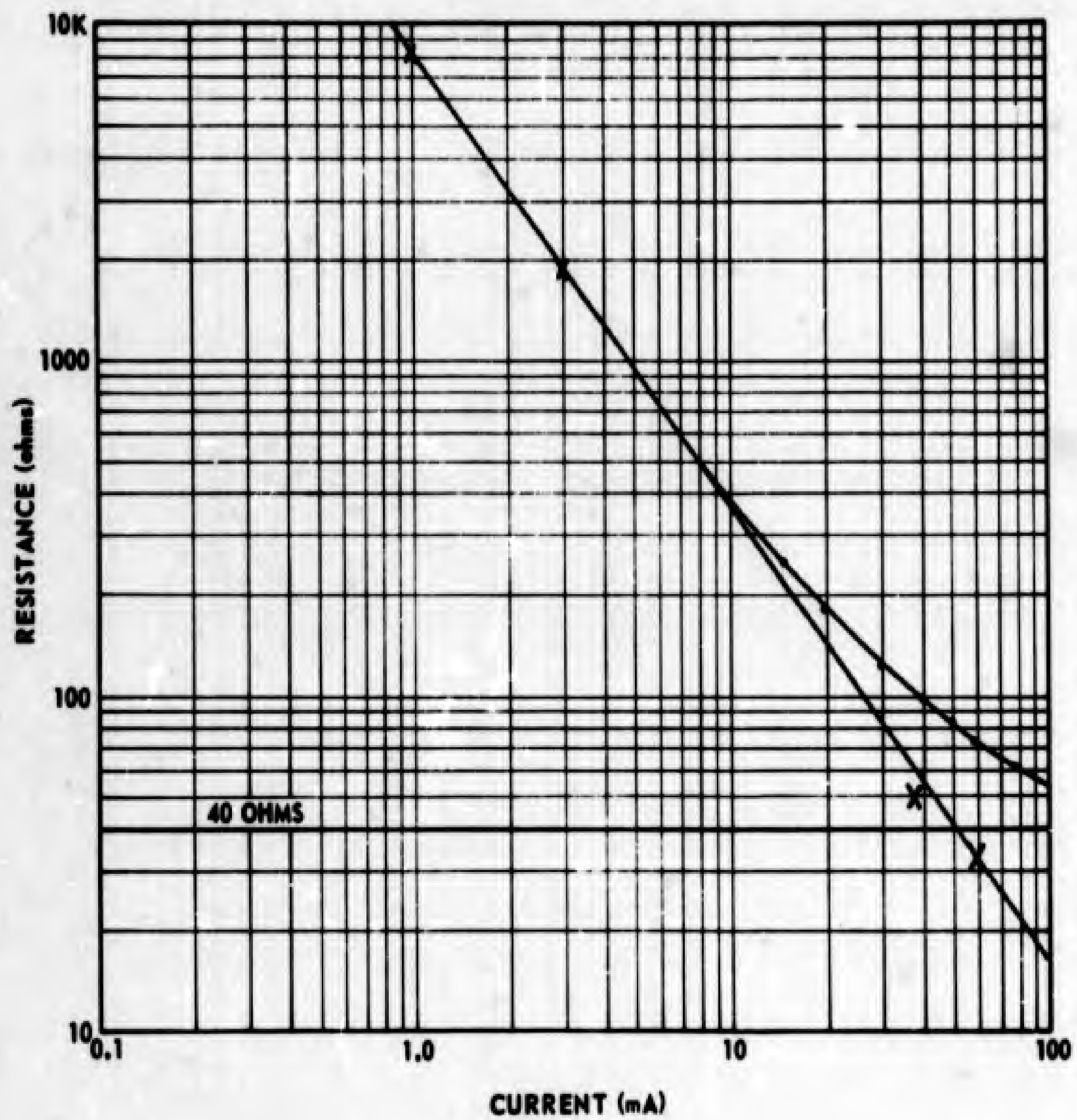

Figure 34. Corrected Characteristic Curve for Bar-Type Unijunction
1.7×10^{12} Neutrons per Square Centimeter

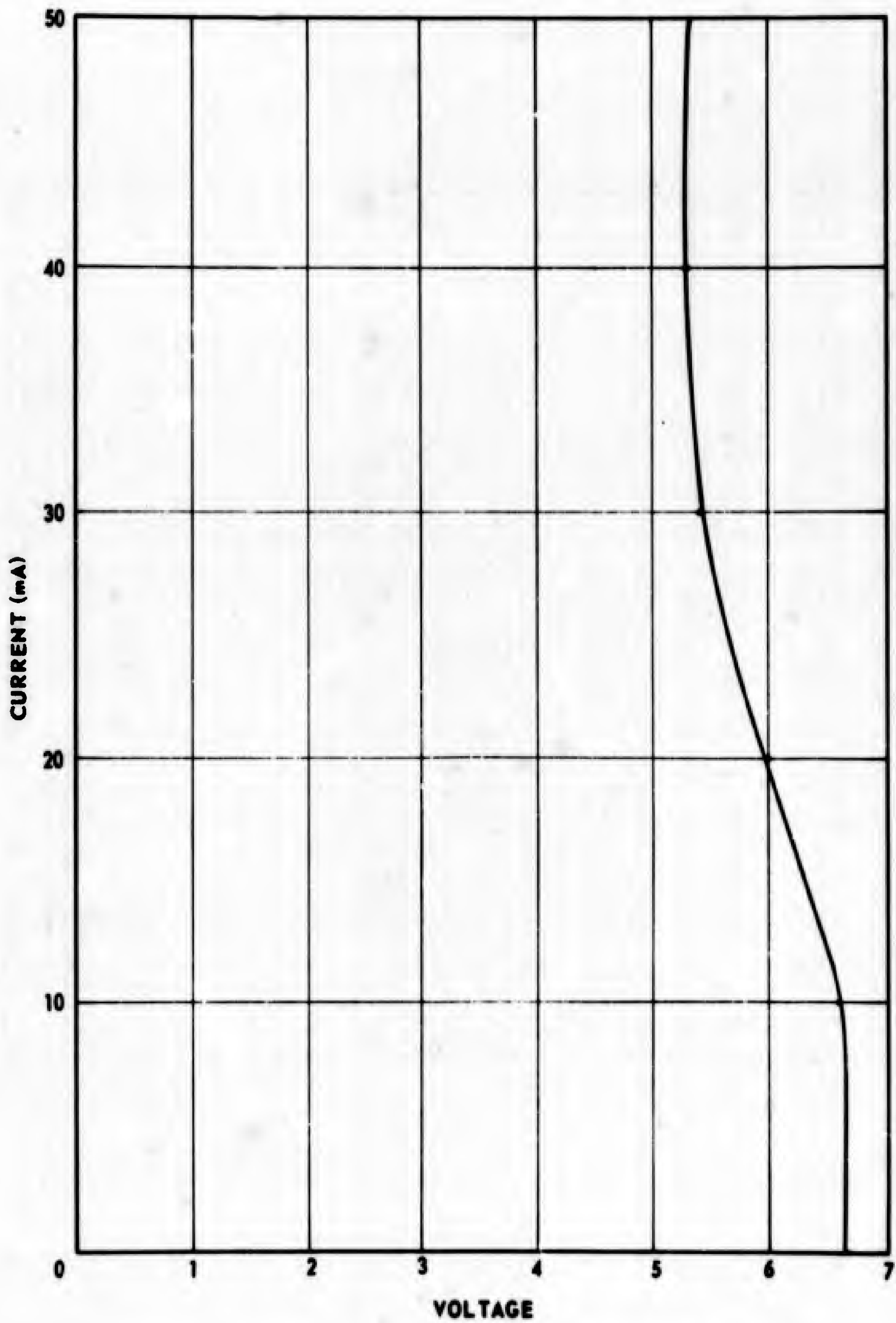

Figure 35. Corrected Voltage-Current Characteristic Curve for Bar-Type Unijunction 1.7 × 10^{12} Neutrons per Square Centimeter

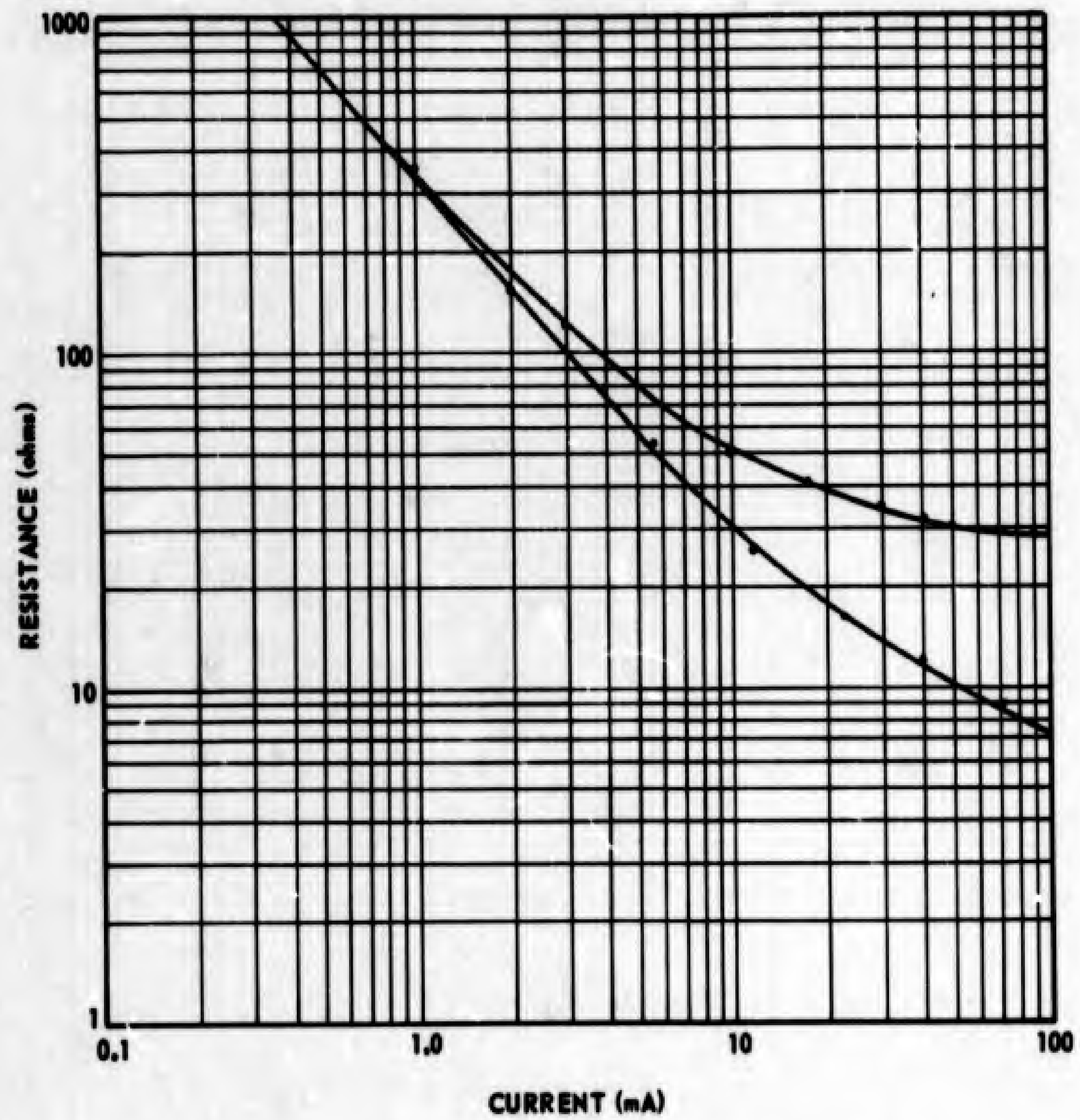

Figure 36. Corrected Composite Curve for Monolithic-Type Unijunction

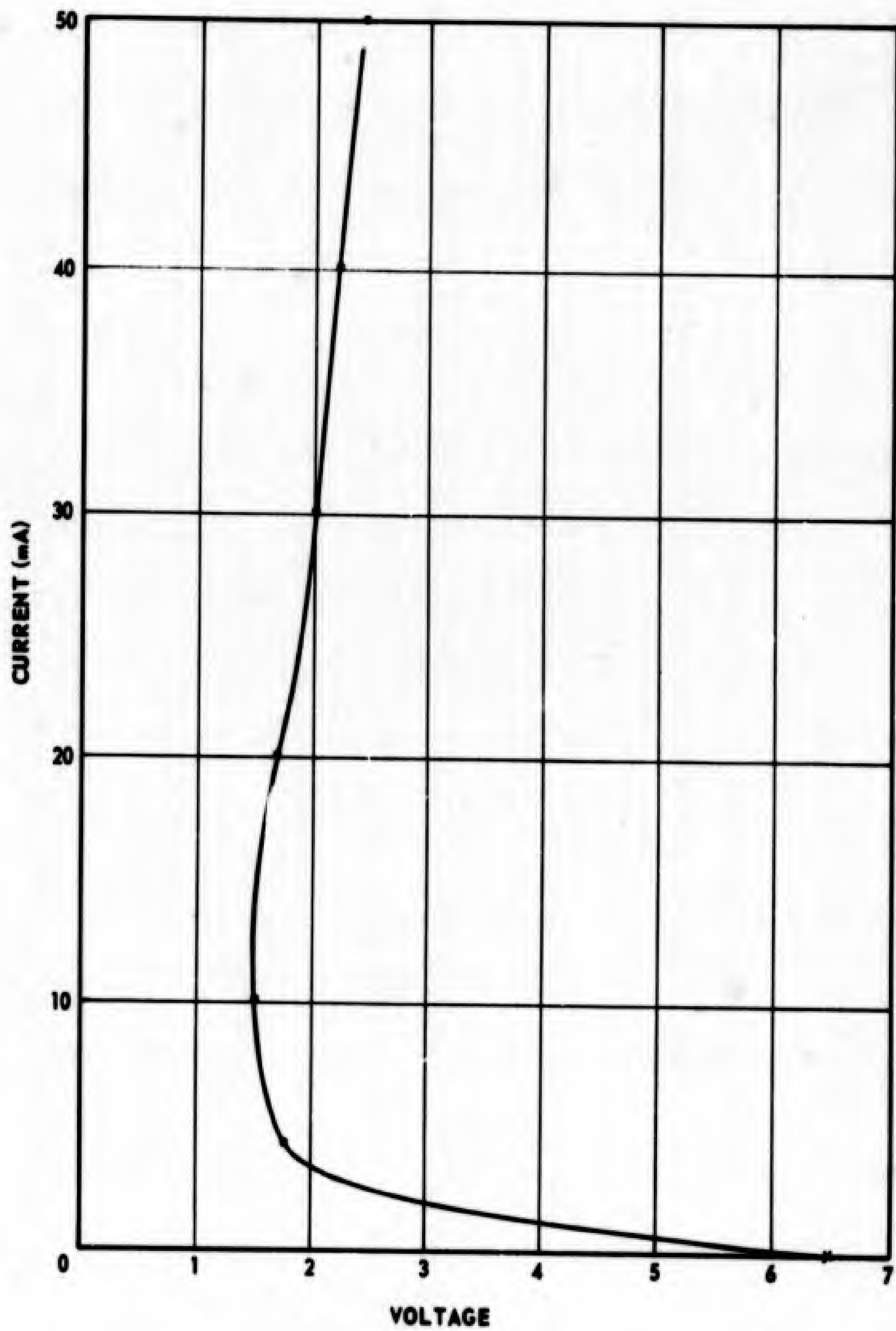

Figure 37. Corrected Voltage-Current Characteristic Curve for Monolithic-Type Unijunction

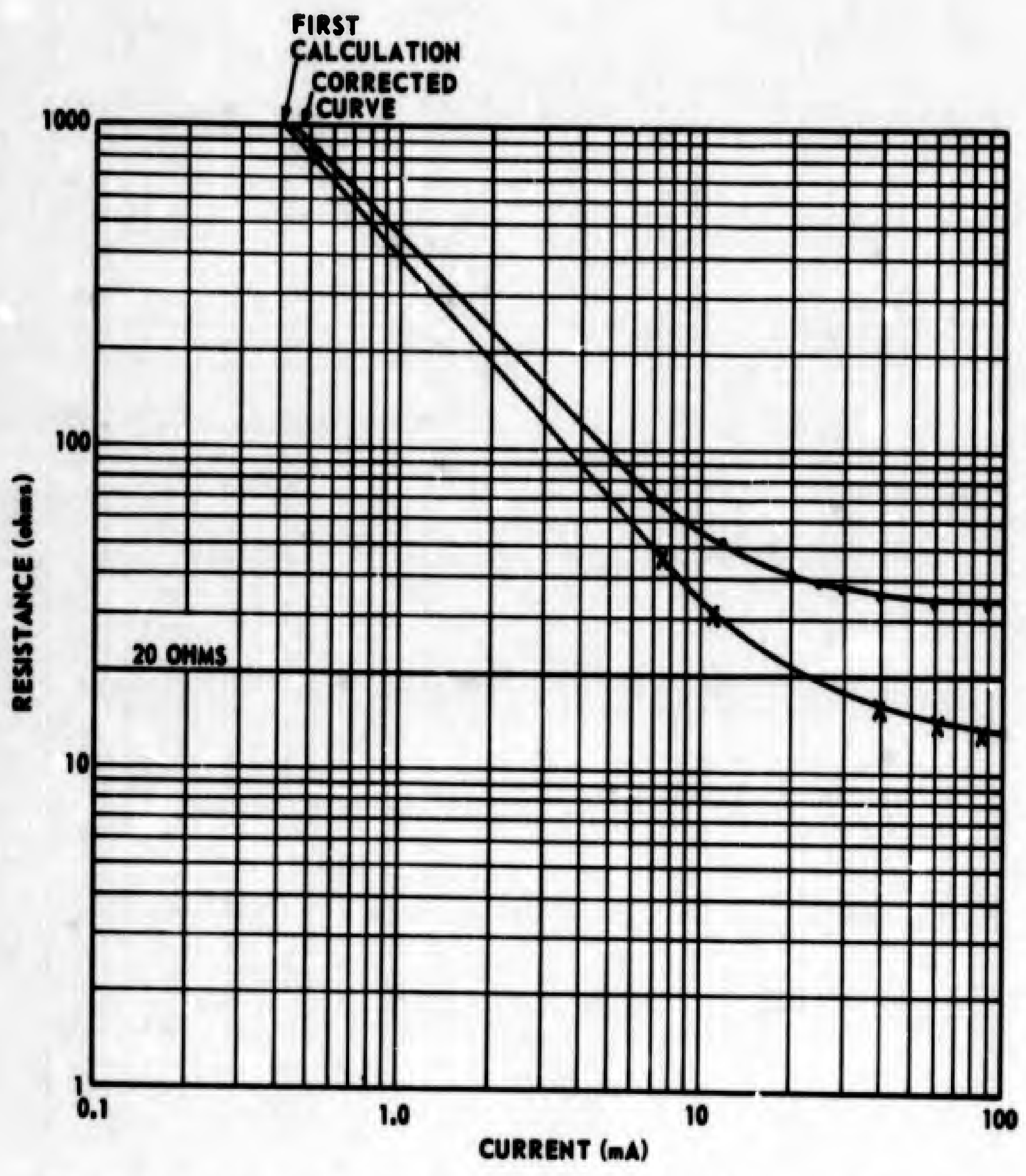

Figure 38. Corrected Composite Curve for Monolithic-Type Unijunction 7.3×10^{12} Neutrons per Square Centimeter

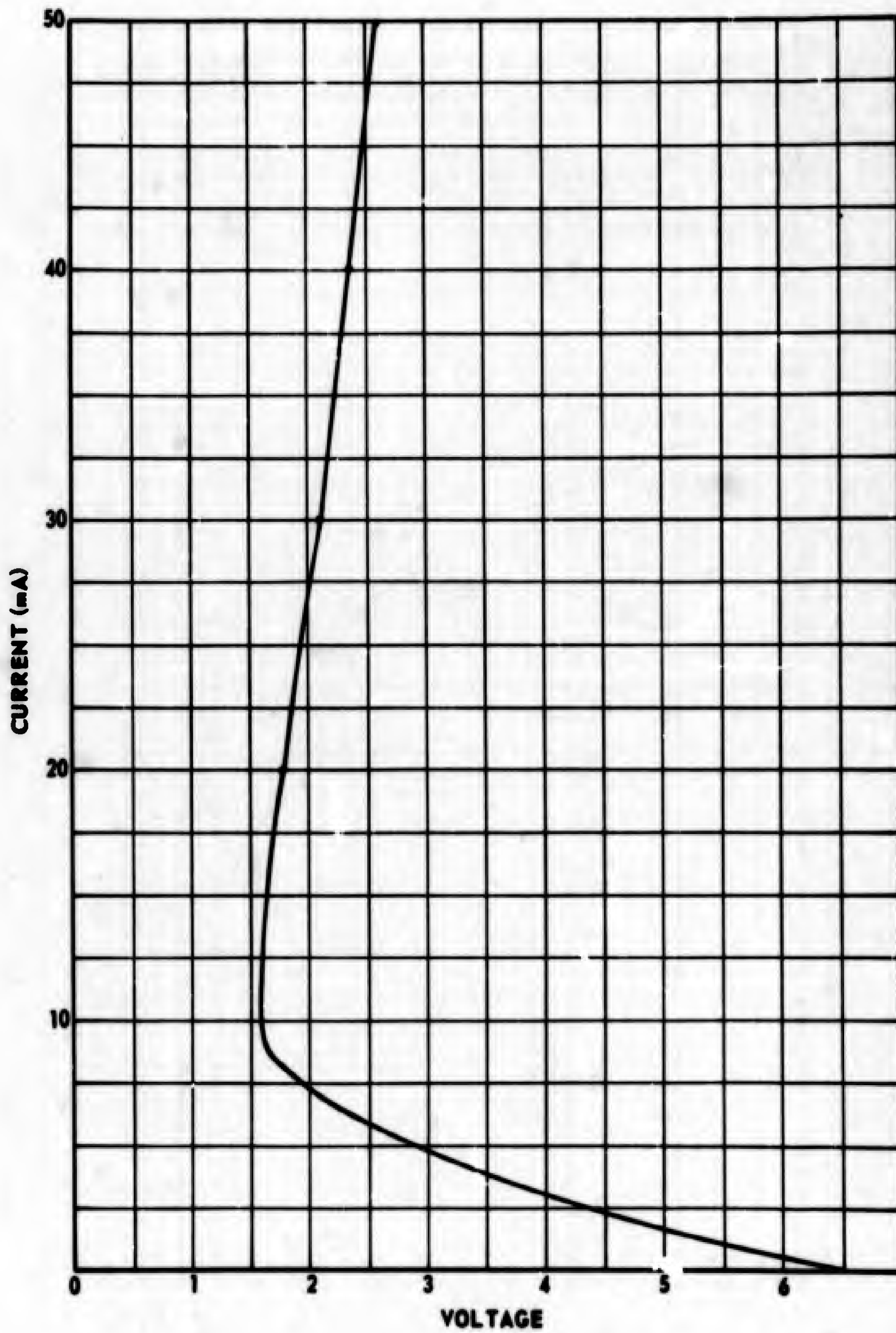

Figure 39. Corrected Voltage-Current Characteristic Curve for Monolithic-Type Unijunction 7.3×10^{12} Neutrons per Square Centimeter

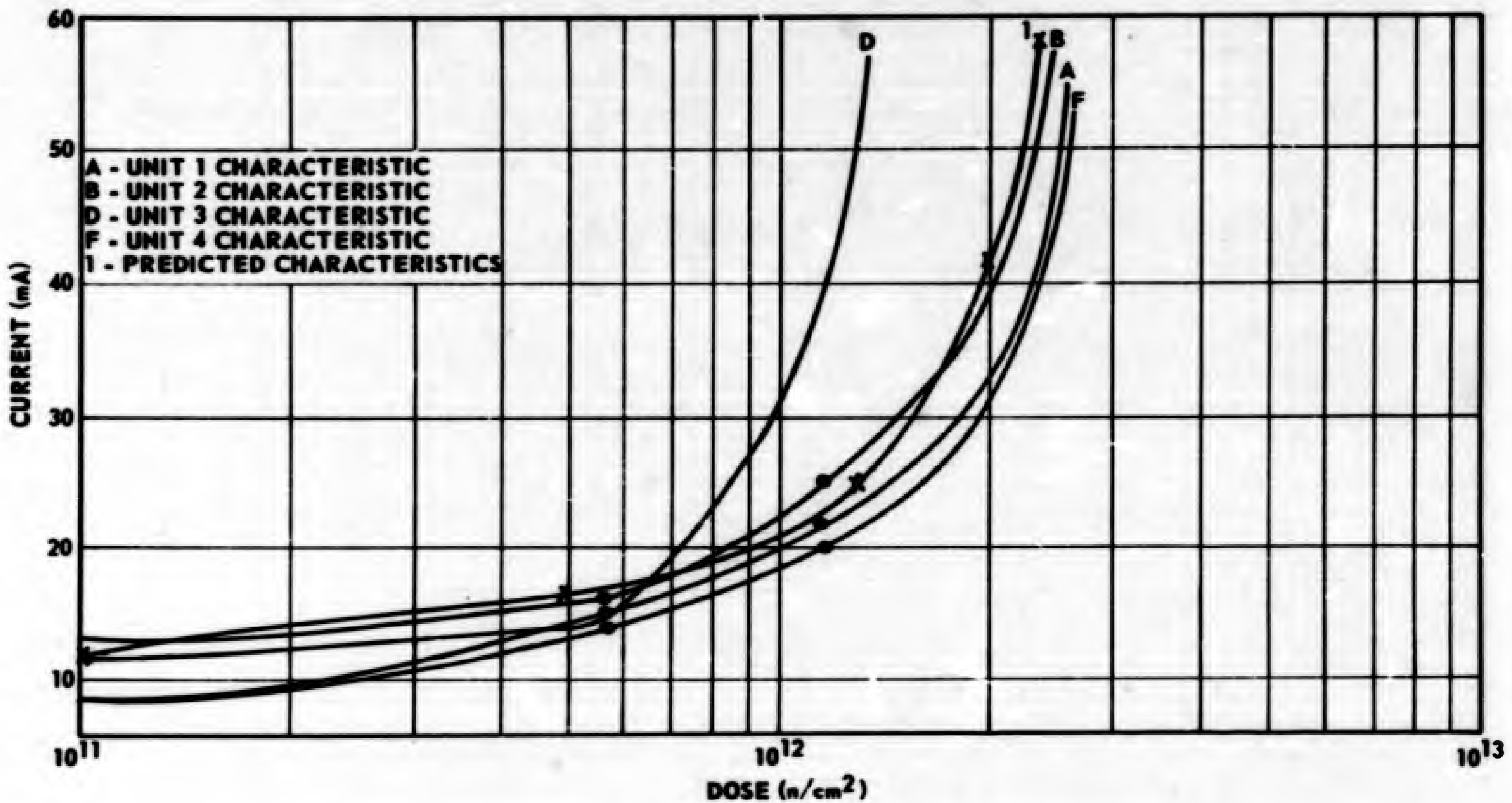

Figure 40. Current-Dose Curve for 2N1772 Silicon Control Rectifier

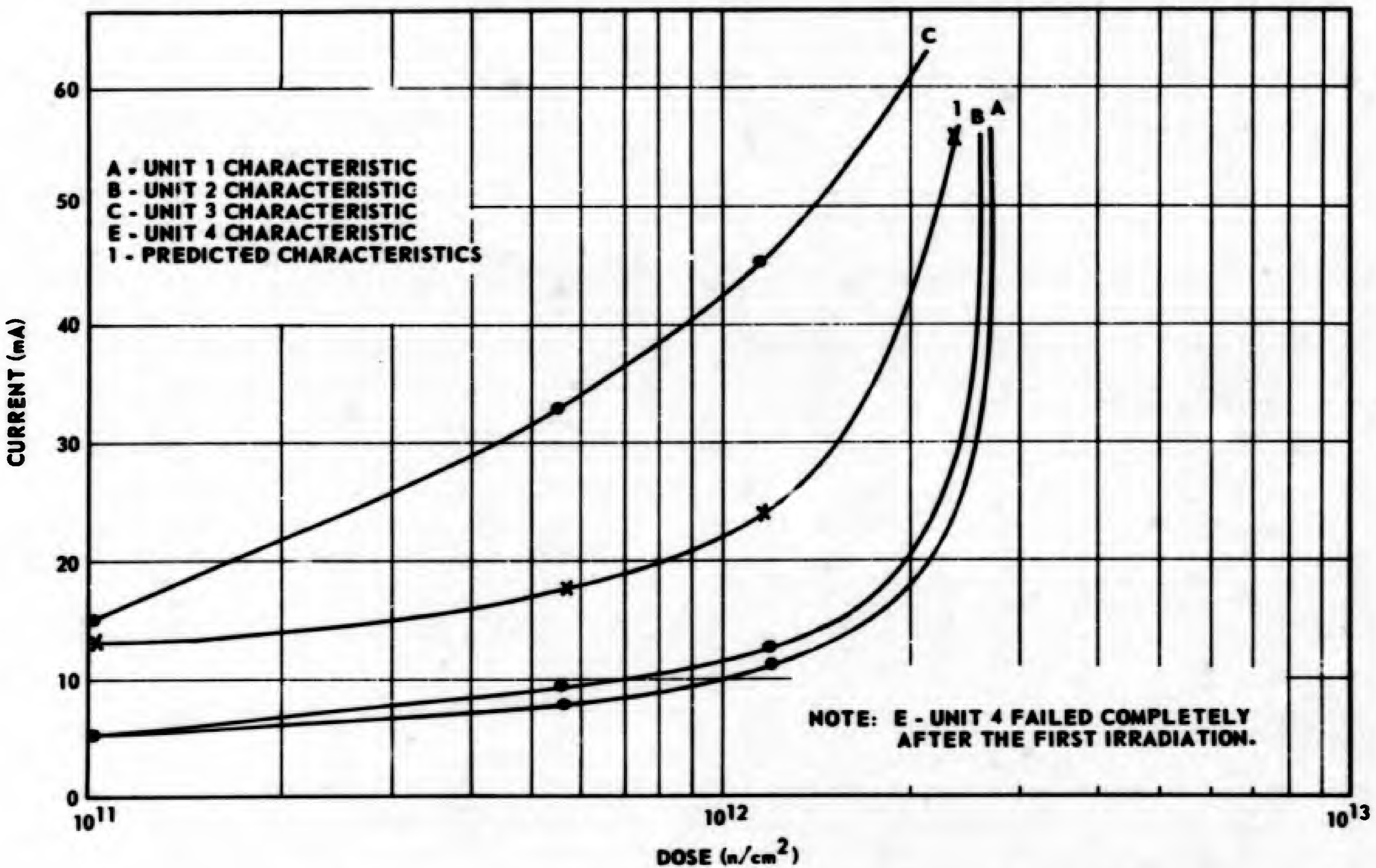

Figure 41. Current-Dose Curve for 2N1843 Silicon Control Rectifier

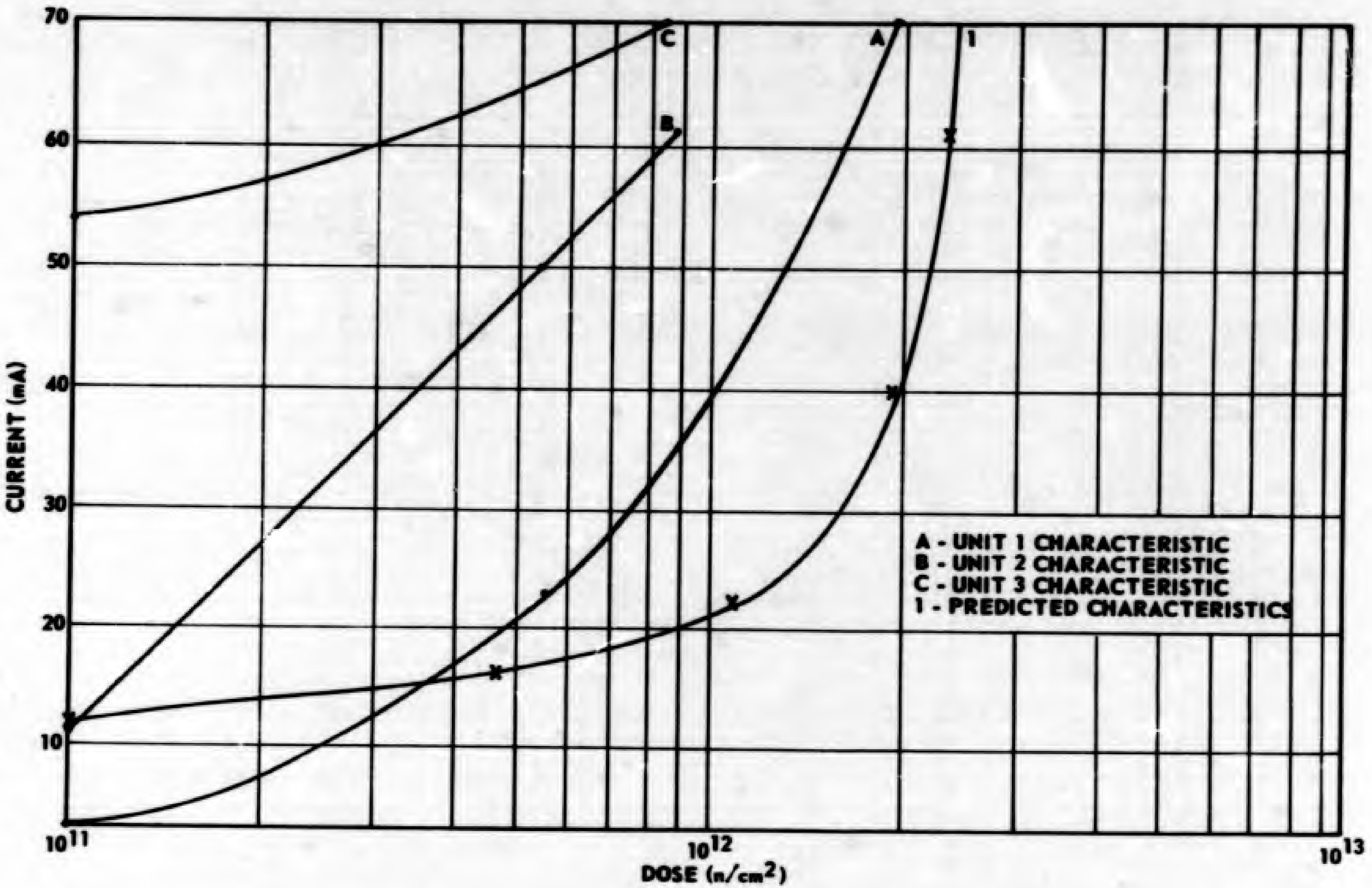

Figure 42. Current-Dose Curve for 2N1595 Silicon Control Rectifier

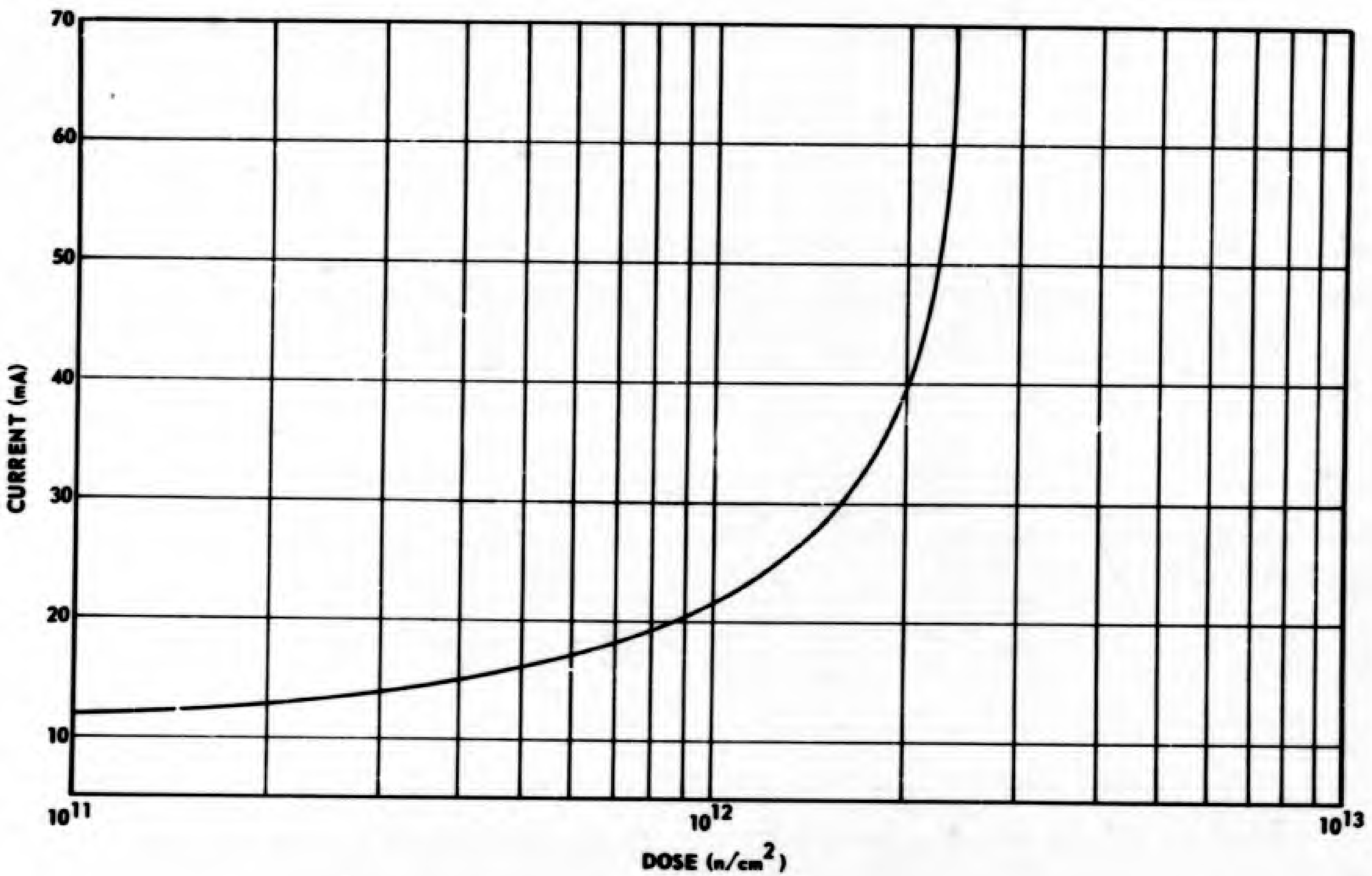

Figure 43. General Prediction Curve for Silicon Control Rectifier

The curve fitting prediction equations are listed in the Appendix. The equation selected for use is

$$I_{SCR} = 0.0145 - 0.00073\,\phi_1 + 0.000113\,\phi_1^2 ,$$

where

$$\phi_1 = (\phi - 10^{11})\ \mathrm{n/cm^2} .$$

CHAPTER V

EFFECT ON CIRCUIT DESIGN

There are two circuits in which unijunctions are commonly employed. These are timing circuits and relaxation oscillators. A typical timing circuit is shown in Figure 44.

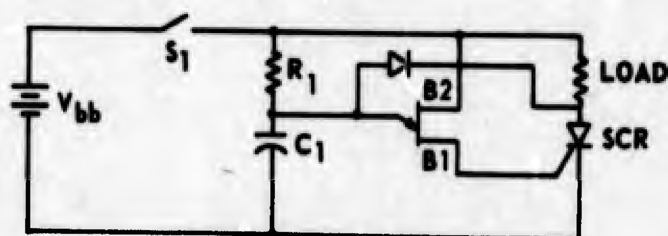

Figure 44. Time Circuit

When S_1 is closed, the capacitor C_1 is charged through Resistor R_1. When the voltage across the capacitor C_1 reaches the firing voltage of the unijunction, the transistor thus conducts and the capacitor discharges through the emitter base 1 junction and through the SCR gate circuit. If the current is of sufficient magnitude and of a sufficient pulse duration, the SCR will be turned on. A neutron environment has direct effect on the characteristic of both the unijunction and the SCR. Neutron radiation causes the base 1 to

emitter resistance to increase, thus reducing the amplitude and duration of the current pulse. This same radiation causes the SCR to require more current and for a longer time.

Consider the model in Figure 45. This represents the unijunction transistor after the device has fired.

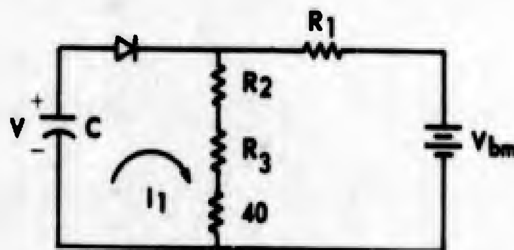

Figure 45. Corrected Unijunction Model

The loop equations can be written as

$$V = \frac{1}{C}\frac{di}{dt} - V_D + (I_1 - I_2)(R_2 + R_3 + 40)$$

$$-V_{bb} = I_2R_1 + (I_2 - I_1)(R_2 + R_3 + 40) \quad . \qquad (5\text{-}1)$$

Sample solutions to these equations for no radiation in a bar-type unijunction are shown in Figure 46. These curves are for 0.1-, 1-, and 10-μf capacitors.

By utilizing the prediction technique, a valley voltage can be predicted. Once the valley voltage or current has been established and the expression for the internal impedance has been developed, the discharge characteristics of the capacitor through the unijunction can be established. From these discharge characteristics, it is possible to determine if there will be sufficient current to turn on the SCR.

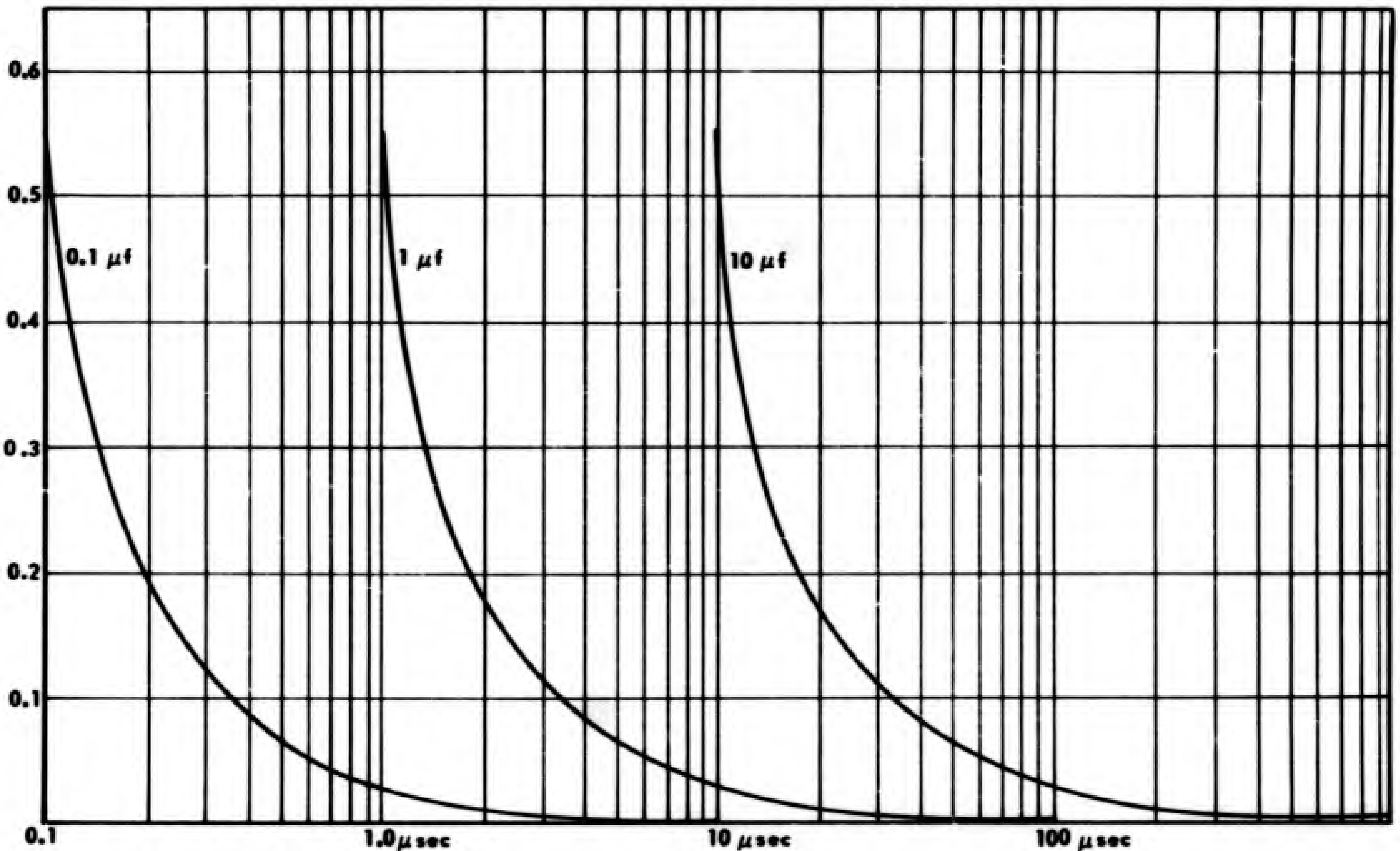

Figure 46. Capacitor Discharge Curve for Nonradiated Case Bar-Type Unijunction

A typical relaxation oscillator is shown in Figure 47.

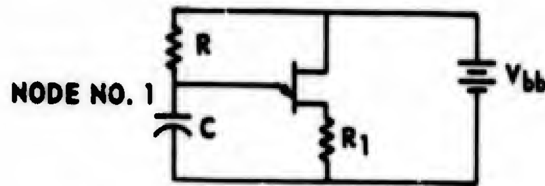

Figure 47. Relaxation Oscillator

The wave shape at node No. 1 is shown in Figure 48.

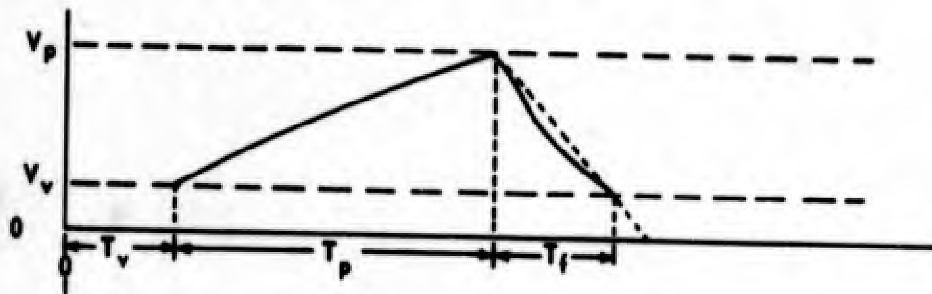

Figure 48. Input Wave Shape

To find the time required to charge capacitor C from zero to the unijunction firing voltage V_f, the following equation for V_f can be solved for t_p

$$V_f = V_{bb}\left(1 - e^{-\frac{t_p}{RC}}\right)$$

$$14 = 20\left(1 - e^{-\frac{t_p}{3.6 \times 10^{-5}}}\right)$$

$$t_p = 3.7 \times 10^5 \ . \qquad (5\text{-}2)$$

In the relaxation oscillator after the first cycle, the capacitor voltage does not charge from a zero level but from the unijunction valley voltage. The

time to charge from zero to V_v can be obtained from the equation for V_v.

$$V_v = V_{bb}\left(1 - e^{-\frac{t_v}{RC}}\right)$$

$$V_v = 20\left(1 - e^{-\frac{t_v}{3.6 \times 10^{-5}}}\right)$$

$$t_v = 3.6 \times 10^{-5} \ln\frac{20}{20 - V_v} . \qquad (5\text{-}3)$$

From equation (5-1), the discharge time can be derived and expressed as

$$T_f = (R_2 + R_3 + 40)C \ln\frac{V_p}{V_v} . \qquad (5\text{-}4)$$

In general, the frequency of oscillation can be written as

$$f = \frac{1}{\left[RC \ln\left(\frac{V_{bb}}{V_{bb} - V_p}\right)\right] - \left[RC \ln\left(\frac{V_{bb}}{V_{bb} - V_v}\right)\right] + \left[(R_2 + R_3 + 40)C \ln\frac{V_p}{V_v}\right]} . \qquad (5\text{-}5)$$

If T_f is assumed small, the frequency changes in this oscillator can be attributed to the change in valley voltages. Such an assumption allows equation (5-5) to be reduced to

$$f = \frac{1}{RC \ln\left(\frac{V_{bb} - V_v}{V_{bb} - V_p}\right)} . \qquad (5\text{-}6)$$

By predicting the voltage-current characteristics and determining the valley voltage at a particular radiation level, an evaluation of the frequency

change can be made.

Consider an oscillator as shown in Figure 47. In the previous case, the supply voltage was assumed to remain constant. However, a variation in this voltage causes a change in the firing voltage. When the voltage V_{bb} is raised the firing voltage will also rise, thus increasing the energy stored in capacitor C. The saturation resistance emitter-base junction is dependent on the current being driven through this junction. This means that by operating at a higher supply voltage, the oscillator will continue to operate at higher levels of radiation. Timers that depend only on the firing voltage can be made to operate to levels of 10^{13} neutrons per square centimeter.

In support of this statement, a circuit was connected as shown in Figure 47 with R = 270,000 ohms, C = 22 microfareds, and R_1 = 47 ohms. An oscilloscope was connected from node No. 1 to ground and the voltage V_{bb} varied between 10 and 28 volts. A number of 2N492 unijunction transistors that were irradiated at 1.7×10^{12} neutrons per square centimeter were placed in this circuit. The oscilloscope photographs of one of these units is shown in Figure 49. These photographs indicate that higher supply voltages V_{bb} provide greater differences between firing voltage and valley voltage. Thus it follows that unijunction transistors should be operated near maximum rated voltage in order to provide maximum hardness to radiation.

Further studies should probably be carried on in order to determine changes in oscillators at high supply voltage. The present data indicate that by operation of an oscillator with a higher supply voltage the effect of neutron damage on its frequency of oscillation would be reduced.

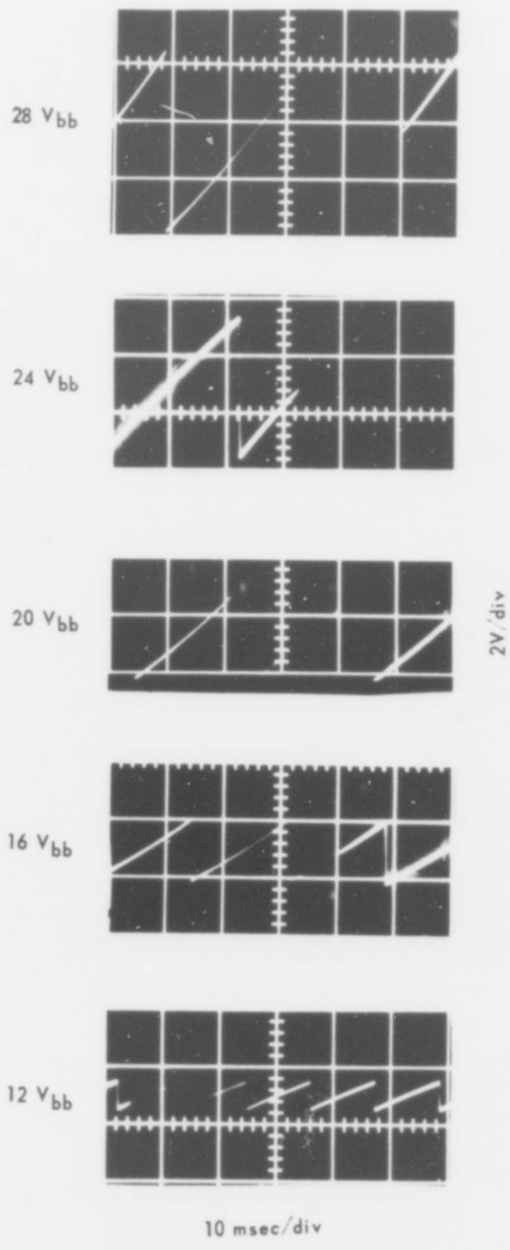

Figure 49. Change in Operational Characteristic for Unijunction with Changes in Supply Voltage

CHAPTER VI

CONCLUSIONS

Unijunction transistors and silicon controlled rectifiers are not the best behaved components, even in the unirradiated state. Unit-to-unit variations are often large and only a general prediction can be made as to the effect radiation will have on a particular circuit. The two types of unijunction transistors in common use are the bar-type and the monolithic-type. Neutron radiation has a greater effect on the bar-type than the monolithic because of the larger volume of silicon used in the bar-type.

The unijunction's two characteristics that are generally employed in circuitry are the valley voltage and firing voltage. The firing voltage is apparently not affected by radiation. Circuits that are only dependent on the firing voltage can be expected to function until the valley voltage is approximately equal to the firing voltage. When such voltage equality occurs, the usefulness of the device is destroyed. This occurs at a dose level of 2×10^{12} neutrons per square centimeter for the bar type and 10^{13} neutrons per square centimeter for the monolithic type. The circuit that depends on the firing voltage characteristics usually contains an SCR. Careful consideration must be given to the interfacing of these semiconducting devices because the

SCR requires a longer pulse length at a larger amplitude after being irradiated, while the unijunction tends to deliver less current at a shorter pulse width.

The valley voltage is a direct function of dose level, and, for this reason, circuits that are dependent on both the firing and valley voltage characteristics are affected more severely by radiation than those dependent on the firing voltage. The change in frequency of a relaxation oscillator can be predicted as a function of valley voltage. This type of oscillator will not operate with the bar-type unijunction transistor above 10^{12} neutrons per square centimeter or with the monolithic above 7×10^{12} neutrons per square centimeter.

A theoretical development was made leading to a prediction technique for the effect of neutron damage on unijunction transistors. It was found that this prediction technique works, in general, but considering the unit-to-unit variation, this method is accurate to within about 10 percent.

The SCR can be made to work in environments up to 2×10^{12} neutrons per square centimeter with increased driving current and pulse width. The unijunction pulse width is adequate and is not affected operationally at this level, therefore good design practices will assure sufficient pulse width. Care must be taken to assure that sufficient current is available to turn on the SCR.

A unijunction circuit can be made harder by operating the device near its maximum voltage. In the oscillator case, changes in frequency due to a particular neutron dose will be less and the oscillator will continue to operate at higher levels of radiation.

In recent years, the computer aided analysis has become of significant importance in the electrical engineering field. Circuit performance under radiation conditions can be predicted by using these programs if an accurate model can be developed. In this thesis, all the necessary ground work has been laid so that a model can be developed. This author feels that additional work should be done to develop a radiation model of a unijunction that will work in the E.C.A.P. and SCEPTRE Computer Programs.

APPENDIX

CHARACTERISTIC CURVE FITTING FOR THE SILICON CONTROL RECTIFIER

The series listed below was selected as the general equation for the Silicon Control Rectifier in a radiation environment. Eight computer runs were made to select the coefficient for this series, and the results of these runs are contained on the following pages (Tables A-I through A-IV).

$$f_{(t)} = A_0 + A_1X + A_2X^2 + A_3X^3 + \ldots$$

The SCR characteristic from which this function was approximated is shown in Figure 43.

Table A-I. Input Data for Silicon Control Rectifier Curve Fitting

Radiation Dose	Current
0.10000000D 01	0.11700000D-01
0.20000000D 01	0.13200000D-01
0.50000000D 01	0.16400000D-01
0.10000000D 02	0.21000000D-01
0.15000000D 02	0.29000000D-01
0.20000000D 02	0.41000000D-01
0.22000000D 02	0.50000000D-01
0.24000000D 02	0.68000000D-01

Table A-II. Output Data for Three Terms

Aj	Value
A 2	0.11378685D-03
A 1	-0.73335913D-03
A 0	0.14547428D-01

Table A-III. Output Data for Four Terms

Aj	Value
A 3	0.10207602D-04
A 2	-0.26649547D-03
A 1	0.29230303D-02
A 0	0.83902432D-02

Table A-IV. Output Data for Five Terms

Aj	Value
A 4	0.70450034D-06
A 3	-0.25350060D-04
A 2	0.30929978D-03
A 1	-0.25983777D-03
A 0	0.12182874D-01

REFERENCES

1. M. Ference, H. B. Lemen, and R. J. Stephenson, Analytical Experimental Physics, University of Chicago Press, 1956, pp. 571-594.

2. Samuel Glasstone, The Effects of Nuclear Weapons, United States Department of Defense, 1962, pp. 369-531.

3. Dale C. Jones, ed., Transient Radiation Effects on Electronics Handbook, Second Edition, Columbus, Ohio, Battelle Memorial Institute, pp. F11-F68.

4. General Electric Co., General Electric Transistor Manual, Fifth Edition, Liverpool, New York, 1960.

5. E. G. Wikner, Displacement Radiation Effects, U. S. Air Force Report, 1961, Contract No. AF 29(601)-4331.

6. R. G. Behrens, Effects of Fast Neutrons on Circuitry Employing Semiconductor Devices, U. S. Air Force Report, November 1957, Contract No. AF 33(600)-24020.

7. D. A. Hicks, D. V. Keller, et al., Radiation Damage to Transistors, U. S. Air Force Report, December 1958, Contract No. AF 33(600)-35030.

8. Harold B. Almond, Fast Neutron Damage to Selected Semiconductor Devices, D2-7427, U. S. Department of Defense Report, October 4, 1960.

9. G. L. Kiester, Permanent Radiation Effects to Electronic Parts and Materials, D2-6595, Vol. I and II, February, 1961.

10. H. M. James and K. Lark-Horovitz, Z. Physik. Chime, 198, No. 107, 1951.

11. V. S. Vavilov, A. V. Spitsyn, L. S. Smirnov, and M. V. Chukichev, J. Exptl. Theoret. Phys., 32, No. 702, 1959

12. Prediction of Transient Nuclear Radiation Effects in Electronic Circuits, D2-9878, January, 1962, Contract No. AF 33(616)-7804.

13. Frank Larin, Seminar Note on Prediction of Radiation Effect in Semiconductor Devices, Seminar on Radiation Effect held at Army Missile Command, Redstone Arsenal, Alabama 35809, 1966.

14. Albert Van Der Ziel, Solid State Physical Electronics, New York, Prentice-Hall, Inc., 1957, pp. 19-103, 241-337.

DOCUMENT CONTROL DATA - R & D

(Security classification of title, body of abstract and indexing annotation must be entered when the overall report is classified)

Field	Entry
1. ORIGINATING ACTIVITY (Corporate author)	Army Inertial Guidance and Control Laboratory and Center Research and Development Directorate U. S. Army Missile Command Redstone Arsenal, Alabama 35809
2a. REPORT SECURITY CLASSIFICATION	Unclassified
2b. GROUP	N/A
3. REPORT TITLE	THE EFFECT OF NEUTRON RADIATION ON UNIJUNCTION TRANSISTORS AND SILICON CONTROL RECTIFIERS
4. DESCRIPTIVE NOTES (Type of report and inclusive dates)	None
5. AUTHOR(S) (First name, middle initial, last name)	Victor W. Ruwe
6. REPORT DATE	14 August 1968
7a. TOTAL NO. OF PAGES	95
7b. NO. OF REFS	0
8a. CONTRACT OR GRANT NO.	
b. PROJECT NO.	
c.	
d.	
9a. ORIGINATOR'S REPORT NUMBER(S)	RG-TR-68-11
9b. OTHER REPORT NO(S) (Any other numbers that may be assigned this report)	AD____________
10. DISTRIBUTION STATEMENT	This document is subject to special export controls and each transmittal to foreign governments or foreign nationals may be made only with prior approval of this Command, ATTN: AMSMI-RG.
11. SUPPLEMENTARY NOTES	None
12. SPONSORING MILITARY ACTIVITY	Same as No. 1.

13. ABSTRACT

~~Presented in this~~ This paper ~~are~~ presents the results of theoretical study and of actual tests on unijunction transistors in a nuclear environment of fast neutrons. The investigation of Silicon Control Rectifiers was principally restricted to their use with unijunction transistors.

In the theoretical study, a technique was developed to predict damage caused by neutrons. A number of sample unijunction transistors were irradiated, then tested, and the results compared with predicted values. It was found that the construction of the device was important in determining the level of radiation that the device could withstand. This study indicates that the monolithic device can be expected to operate in neutron environments about five times higher than the bar type device and the Silicon Control Rectifiers.

DD FORM 1 NOV 65 1473 REPLACES DD FORM 1473, 1 JAN 64, WHICH IS OBSOLETE FOR ARMY USE.

14. KEY WORDS	LINK A		LINK B		LINK C	
	ROLE	WT	ROLE	WT	ROLE	WT
Unijunction transistors						
Silicon Control Rectifiers						
Neutron radiation						